International Journal for Parasitology

The key to egress? Babesia bovis perforin-like protein 1 (PLP1) with hemolytic capacity is required for blood stage replication and is involved in the exit of the parasite from the host cell.

--Manuscript Draft--

Manuscript Number:	IJPara20_284R2
Article Type:	Full Length Article
Keywords:	Babesia bovis; perforin-like protein; transfection; hemolysis assay; membrane attack complex/perforin (MACPF) domain; pore forming protein
Corresponding Author:	Silvina E Wilkowsky, Ph.D Consejo Nacional de Investigaciones Cientificas y Tecnicas Hurlingham, Buenos Aires ARGENTINA
First Author:	Martina Soledad Paoletta
Order of Authors:	Martina Soledad Paoletta
	Jacob Michael Laughery
	Ludmila Sol López Arias
	José Manuel Jaramillo Ortiz
	Valeria Noely Montenegro
	Romina Petrigh
	Massaro W. Ueti
	Carlos Esteban Suarez
	Marisa Diana Farber
	Silvina E Wilkowsky, Ph.D
Abstract:	Bovine babesiosis is a tick-borne disease caused by apicomplexan parasites of the Babesia genus that represents a major constraint to livestock production worldwide. Currently available vaccines are based on live parasites which have archetypal limitations. Our goal is to identify candidate antigens so that new and effective vaccines against Babesia may be developed. The perforin-like protein (PLP) family has been identified as a key player in cell traversal and egress in related apicomplexans and it was also identified in Babesia , but its function in this parasite remains unknown. The aim of this work was to define the PLP family in Babesia and functionally characterize PLP1, a representative member of the family in B. bovis . Bioinformatic analyses demonstrate a variable number of plp genes (4 to 8) in the genomes of six different Babesia species and conservation of the family members at the secondary and tertiary structure levels. We demonstrate here that Babesia PLPs contain the critical domains present in other apicomplexan PLPs to display the lytic capacity. We then focused on the functional characterization of the PLP1 protein of B. bovis, both in vitro and in vivo . PLP1 is expressed and exposed to the host immune system during infection and has high hemolytic capacity in a wide range of conditions in vitro . A B. bovis plp1 knock out line displayed decreased growth rate in vitro compared to the wild type strain and a peculiar phenotype consisting of multiple parasites within a single RBC, although in low frequency. This phenotype suggests that the lack of PLP1 has a negative impact on the mechanism of egression of the parasite and, therefore, in its capacity to proliferate. It is possible that PLP1 is associated with other proteins in the processes of invasion and egress, which were found to have redundant mechanisms in related apicomplexans. Future work will be focused on unravelling the network of proteins involved in these essential parasite functions.

Buenos Aires, June 19th, 2020.

International Journal for Parasitology

Editor-in-Chief

B. M. Cooke

Dear Editor,

Please find enclosed the manuscript entitled "**The key to escape? *Babesia bovis* perforin-like protein 1 (PLP1) with hemolytic capacity is required for blood stage replication and is involved in the egress of the parasite from the host cell"** by Dr. Martina S. Paoletta and collaborators.

This article deals with the identification and characterization of the members of the perforin-like protein (PLP) family in parasites of the *Babesia* genus, focusing in both their structure and function. *Babesia* are tick-borne protozoan parasites that represent a major constraint to livestock production worldwide. Our goal is to identify candidate antigens to develop new and effective vaccines against *Babesia.* In this sense, the PLP family has proven to be a key player in life cycle progression in related apicomplexans, but its function in *Babesia* parasite remains unknown.

In this paper, we identified *plp* coding genes in different *Babesia* species and characterized their genomic organization, pattern of expression and evolutionary relationships. Furthermore, we performed an *in vitro* functional characterization of *B. bovis* PLP1, a representative member of the family, which displayed high hemolytic capacity in a wide range of conditions. We have also generated a *plp1* knock out line that showed an abnormal phenotype and a diminished growth rate compared to the wild type strain. Overall, our results demonstrate that PLP1 is not essential but plays an important role in the egression of the parasite from the host cell.

Further *in vivo* studies with the *plp1* knock out line will allow us to analyze if the *in vitro* replication defect results in an attenuated phenotype, which can be of great value since knock out strains arise as an alternative to traditional live vaccines.

Instituto de Biotecnología
Instituto de Agrobiotecnología y Biología Molecular – IABiMo – INTA-CONICET
Centro de Investigación en Ciencias Veterinarias y Agronómicas - C.I.C.V.y A.
CNIA – INTA Castelar
Casilla de Correo Nº 25 (Cnel. Martin Irigoyen 484 – CP 1712 Castelar - Bs. As.)
Provincia de Buenos Aires, República Argentina
Teléfonos: +54 11 4621-1447/1676/1127/1278

Please, find below the highlights of this manuscript. I hope you find this work interesting for considering its publication at the International Journal for Parasitology.

I look forward to hearing from you soon.

Yours sincerely,

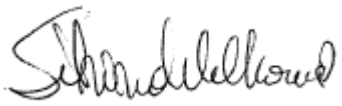

Dr. Silvina E. Wilkowsky
Instituto de Agrobiotecnología y Biología Molecular (IABIMO)
INTA-CONICET
Buenos Aires - ARGENTINA
E-mail: wilkowsky.silvina@inta.gob.ar

Highlights

- All *Babesia* PLPs have the critical domains necessary for pore formation.
- *B. bovis* PLP1 is expressed and exposed to the bovine immune system.
- *B. bovis* PLP1 has high hemolytic capacity in a wide range of conditions.
- A *B. bovis Δplp1* line shows a slower growth rate in *in vitro* cultures.
- Some *Δplp1* parasites accumulate in erythrocytes implying a role of PLP1 in egress.

Reviewers' comments:

Reviewer #1:

I had in my first review asked the authors to test the antiserum (now Fig. S9) against the KO parasite. The purpose is to validate that the antiserum is indeed recognizing the correct protein (not that the KO is correct which they had shown with other methods). My opinion is that this control must be added to Fig. S9.

Response: *We believe that we have already successfully demonstrated the specificity of the antiserum against PLP1 with the assays shown in supplementary figure S9.*

We showed that: [A] Mice antiserum raised against the recombinant MACPF domain of PLP1 (42,4 kDa) recognizes in Western blot analysis a protein with a size that matches the full-length of PLP1 (108 kDa) that is expressed in merozoites of a wild type B. bovis strain (Supplementary Figure S9A, line 3). Pre-immune mice serum does not recognize any antigen in infected erythrocytes. [B] We also demonstrated that the mice antiserum raised against the recombinant MACPF domain of PLP1 reacts with a protein of the exact same molecular weight as the recombinant PLP1_MACPF protein recognized by the commercial anti histidine antibody (Supplementary Figure S9B lines 3 and 4, respectively). [C] We also showed that the recombinant MACPF domain of PLP1 is detected by sera from bovines that were naturally infected with B. bovis (Supplementary Figure S9B, line 2). Clearly this antibody response requires expression of PLP1 in blood stages, during infection.

In summary, three independent lines of evidence are consistently in agreement with our contention that the mice antibodies against the recombinant MACPF domain of PLP1 recognize the native version of the protein, and that PLP1 is expressed in B. bovis merozoites and exposed to the host immune system during infection. In addition, expression of PLP1 in the wild type strain, was also demonstrated upon analysis of global transcriptomic data sets (Figure 4) and further confirmed by RT-PCR analysis (Supplementary Figure S10). We respect the opinion of the reviewer, but we feel that adding an additional Western blot Figure to the manuscript would not serve any additional purposes and it would be redundant.

I have two minor comments that should also be dealt with.

The supplemental figures should be reordered to be consistent with the text (Fig S1 should be mentioned first etc).

Response: *The supplemental figures are already properly ordered in the text, being Figure S1 first mentioned in line 228 (Materials and methods section), followed by Figure S2 in line 259 (Materials and methods section), Figure S3 to S5 in line 340 (Results section), and so on.*

line 539 "in the" repeated twice.

Response: *The sentence was corrected.*

Reviewer #2:

All of my prior comments have been addressed.

This reviewer is only left with one minor question about the hemolysis assay that does not affect the overall conclusions of this manuscript. Most MACPF proteins appear to recognize and bind to the membrane via a C-terminal domain. In apicomplexan parasites this would, presumably, occur via the APCbeta domain. The hemolysis assay presented in this manuscript was performed with only MACPF domain. Do the authors think that the MACPF domain has membrane binding activity that is independent of the APCbeta domain? Or is the hemolysis activity observed part of an adventitious non-canonical pore forming mechanism that is distinct from the mechanism that likely occurs in full length protein secreted from micronemes during egress?

Response: *We hypothesize that, at least in this particular case, the MACPF domain has membrane binding activity on its own, while the APCbeta domain might be responsible for regulation of the protein activity by, for example, calcium binding or regulating polymerization. This hypothesis is based, among other things, on the fact that many Babesia PLPs lack the C-terminal domain and also on hemolysis assays performed by Garg et al., 2013 with Plasmodium falciparum PLP1. The authors showed that both the full-length protein and the isolated MACPF domain had membranolytic activity, where the only difference was that the activity of full-length protein was sensitive to calcium while the MACPF domain was active independently of the presence/absence of the ion.*

These observations contrast with hemolysis assays done on PLP1 of T. gondii (Guerra and Carruthers, 2017; Roiko and Carruthers, 2013) where the APCbeta domain is indispensable for pore formation and, as

discussed in the manuscript, suggest that the APCbeta domain in Hematozoa might play a different role than in Coccidia. However, more experiments should be done to confirm these speculations.

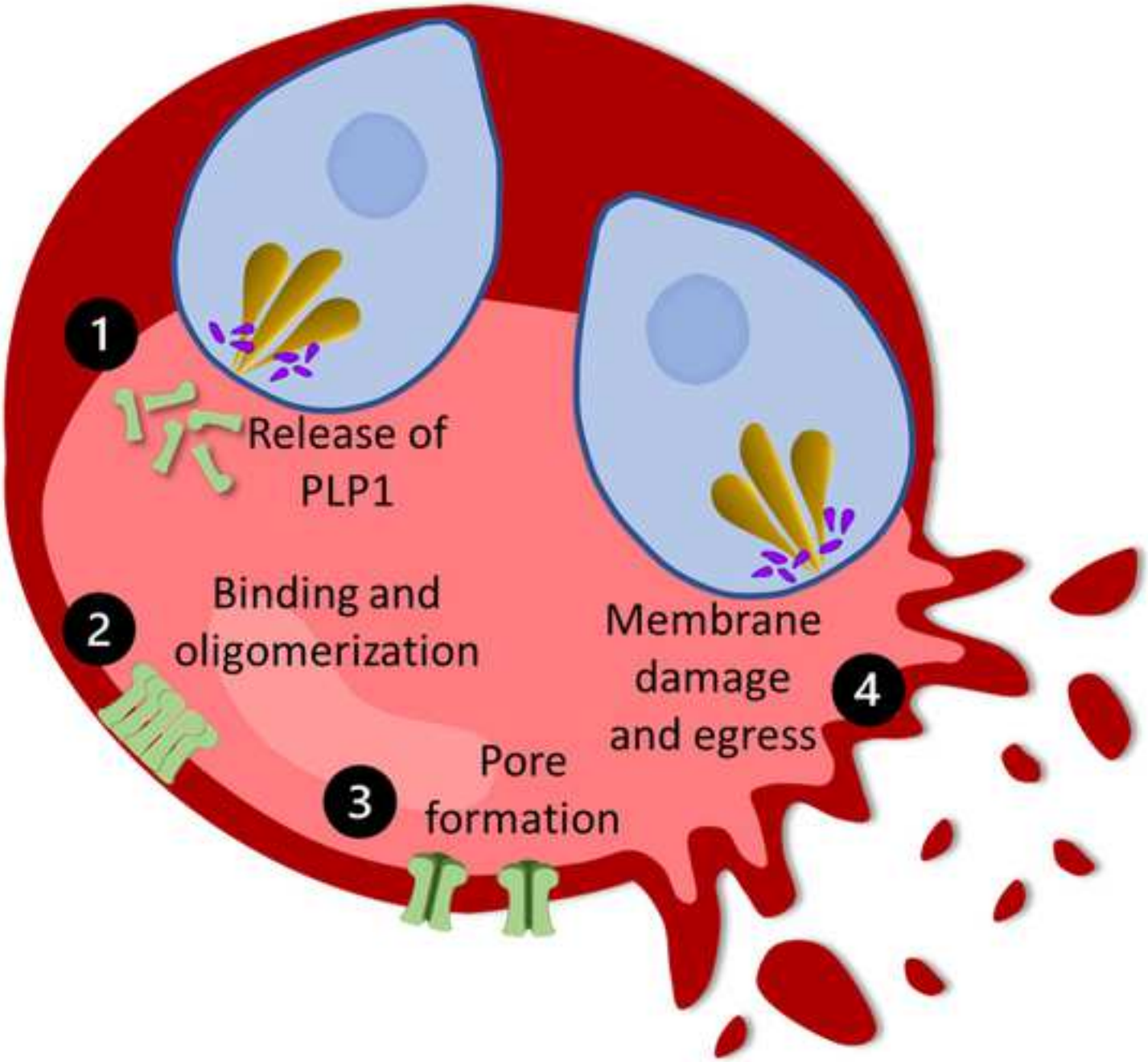

Highlights

- All *Babesia* PLPs have the critical domains necessary for pore formation.
- *B. bovis* PLP1 is expressed and exposed to the bovine immune system.
- *B. bovis* PLP1 has high hemolytic capacity in a wide range of conditions.
- A *B. bovis Δplp1* line shows a slower growth rate in *in vitro* cultures.
- Some *Δplp1* parasites accumulate in erythrocytes implying a role of PLP1 in egress.

The key to egress? *Babesia bovis* perforin-like protein 1 (PLP1) with hemolytic capacity is required for blood stage replication and is involved in the exit of the parasite from the host cell.

Martina Soledad Paoletta[a], Jacob Michael Laughery[b], Ludmila Sol López Arias[a,1], José Manuel Jaramillo Ortiz[a], Valeria Noely Montenegro[a], Romina Petrigh[a,2], Massaro W. Ueti[b,c], Carlos Esteban Suarez[b,c], Marisa Diana Farber[a], Silvina Elizabeth Wilkowsky[a].

[a] Instituto de Agrobiotecnología y Biología Molecular (IABIMO) INTA - CONICET, De Los Reseros y Dr. Nicolás Repetto s/n, P.O. Box 25 (B1712WAA), Castelar, Buenos Aires, Argentina.

[b] Department of Veterinary Microbiology and Pathology, Washington State University, Pullman, WA 99164, USA.

[c] Animal Disease Research Unit, USDA-ARS, Washington State University, 3003 ADBF, P.O. Box 646630, Pullman, WA 99164, USA.

[1] Present address: Universidad Nacional de Hurlingham. Instituto de Biotecnología. Av. Vergara 2222 (B1688GEZ), Villa Tesei, Buenos Aires, Argentina.

[2] Present address: Instituto de Investigaciones en Sanidad, Producción y Ambiente (IIPROSAM), Universidad Nacional de Mar del Plata-CONICET, Dean Funes 3250 (7600), Mar del Plata, Buenos Aires, Argentina.

Corresponding author

Silvina E. Wilkowsky, wilkowsky.silvina@inta.gob.ar.

Instituto de Agrobiotecnología y Biología Molecular (IABIMO) INTA - CONICET, De Los Reseros y Dr. Nicolás Repetto s/n, P.O. Box 25 (B1712WAA), Castelar, Buenos Aires, Argentina.

Note: Supplementary data associated with this article

Abstract

Bovine babesiosis is a tick-borne disease caused by apicomplexan parasites of the *Babesia* genus that represents a major constraint to livestock production worldwide. Currently available vaccines are based on live parasites which have archetypal limitations. Our goal is to identify candidate antigens so that new and effective vaccines against *Babesia* may be developed. The perforin-like protein (PLP) family has been identified as a key player in cell traversal and egress in related apicomplexans and it was also identified in *Babesia*, but its function in this parasite remains unknown. The aim of this work was to define the PLP family in *Babesia* and functionally characterize PLP1, a representative member of the family in *B. bovis*. Bioinformatic analyses demonstrate a variable number of *plp* genes (4 to 8) in the genomes of six different *Babesia* species and conservation of the family members at the secondary and tertiary structure levels. We demonstrate here that *Babesia* PLPs contain the critical domains present in other apicomplexan PLPs to display the lytic capacity. We then focused on the functional characterization of the PLP1 protein of *B. bovis,* both *in vitro* and *in vivo*. PLP1 is expressed and exposed to the host immune system during infection and has high hemolytic capacity in a wide range of conditions *in vitro*. A *B. bovis plp1* knock out line displayed decreased growth rate *in vitro* compared to the wild type strain and a peculiar phenotype consisting of multiple parasites within a single RBC, although in low frequency. This phenotype suggests that the lack of PLP1 has a negative impact on the mechanism of egression of the parasite and, therefore, in its capacity to proliferate. It is possible that PLP1 is associated with other proteins in the processes of invasion and egress, which were found to have redundant mechanisms in related apicomplexans. Future work will be focused on unravelling the network of proteins involved in these essential parasite functions.

Keywords

Babesia bovis, perforin-like protein, transfection, hemolysis assay, membrane attack complex/perforin (MACPF) domain, pore forming protein

1. Introduction

Babesiosis is a tick-borne disease caused by apicomplexan parasites of the *Babesia* genus that replicate within red blood cells (RBC) of a wide range of hosts. Bovine babesiosis is a major constraint to livestock production, affecting more than 500 million cattle annually worldwide (Bock et al., 2004). The two most relevant species affecting cattle are *B. bovis* and *B. bigemina* (Bock et al., 2004), however another bovine species, *B. divergens,* is also gaining increasing interest as an emerging zoonosis of humans (Gohil et al., 2013). The main symptoms of babesiosis are hemolytic anemia and fever, with occasional hemoglobinuria and death (Bock et al., 2004). *B. bovis* is responsible for the most severe form of the disease since it is also capable of changing the structure of the membrane of the infected RBC which leads to their accumulation in the capillaries of different organs and the subsequent development of fatal clinical complications (Gohil et al., 2013). Although vaccine development has been the subject of intense research, to date, the only effective strategy to prevent acute babesiosis in endemic areas is the use of live attenuated vaccines, despite the numerous risks and application drawbacks that these vaccines effectuate (de Waal and Combrink, 2006; Florin-Christensen et al., 2014).

The cycle of replication of *Babesia* parasites in the bovine host involves invasion of RBCs, duplication by binary fission and egress from the host cell. This generates high levels of hemolysis concomitant with a high rate of erythrocyte destruction that contributes to anemia.

The definition of the proteins implicated in life cycle progression of *Babesia* blood stages is of special interest to better understand host-pathogen interactions that will lead to the development of novel and more effective methods to control the disease. While invasion has been studied in more detail and some of the proteins involved have been characterized, the egress process remains poorly understood.

In the past few years, the perforin-like protein (PLP) family has been identified as a key player in cell traversal or egress in apicomplexan parasites such as *Toxoplasma gondii* and various *Plasmodium* species. PLPs are defined by the presence of a membrane attack complex/perforin (MACPF) domain with the ability to form pores in lipid bilayers, and a β-sheet rich domain located in the C-terminal end of the protein, named APC-β which is unique to *Apicomplexa* and might play a role in membrane recognition and binding (Kafsack and Carruthers, 2010; Guerra and Carruthers, 2017; Guerra et al., 2018; Ni et al., 2018).

Apicomplexan PLPs generate membrane pores and play different roles depending on the organism and stage of the life cycle in which they are expressed (Roiko and Carruthers, 2009; Kafsack and Carruthers, 2010; Guerra and Carruthers, 2017). In *T. gondii*, PLP1 allows the tachyzoites to egress from an exhausted host cell to re-invade a new fresh one (Kafsack et al., 2009; Roiko and Carruthers, 2013). In *Plasmodium* sp. some PLPs are involved in egress while others facilitate the movement of the parasite through different epithelia (Kadota et al., 2004; Kaiser et al., 2004; Ishino et al., 2005; Ecker et al., 2007; Amino et al., 2008; Deligianni et al., 2013; Garg et al., 2013; Wirth et al., 2014; Garg et al., 2015; Risco-Castillo et al., 2015; Wirth et al., 2015; Yang et al., 2017; Deligianni et al., 2018; Garg et al., 2020). So far, all characterized PLPs are located in micronemes, an apicomplexan type of secretory organelles that play an important role in the invasion and egress from the host cell, with the exception of *P. berghei* PLP4, which is located in apical vesicles different from micronemes (Deligianni et al., 2018). Furthermore, a recent study on *P. falciparum* has shown that inhibitors that target PLPs restrict pore formation effectively blocking intraerythrocytic growth, as well as the hepatic and transmission stages (Garg et al., 2020).

Despite their perceived functional importance in *Apicomplexa*, the PLP family of *Babesia* spp. parasites remains poorly studied. Even though there is evidence of the presence of *plp* genes and their transcription levels (de Vries et al., 2006; Brayton et al., 2007; Kafsack and Carruthers, 2010; Wade and Tweten, 2015; Moreno-Hagelsieb et al., 2017; Elton et al., 2019; González et al., 2019) thorough structural and functional genomic studies have not been performed yet.

The aim of this study was to identify and characterize the members of the PLP family in parasites of the *Babesia* genus focusing on both their structure and function. Hereby, we have identified a variable number of *plp* coding genes in the genomes of different *Babesia* species and characterized the genomic organization, pattern of expression and evolutionary relationships of their gene families. Based on these and previous data, we have then selected and expressed PLP1 of *B. bovis* for performing *in vitro* and *in vivo* functional characterizations. We have generated a *plp1* knock out (*Δplp1*) line which was viable but displayed an abnormal phenotype and a diminished growth rate compared to the wild type (WT) strain. We demonstrate here that even though the *B. bovis plp1* gene is not essential for the *in vitro* development of

erythrocyte stages, its absence has a negative impact on the mechanism of egression of the parasite and therefore in its proliferative capacity.

2. Material and Methods

2.1 Database search and sequence analysis

The 20 amino acid motif WX(2)[FL][FI]X(2)[FY]GTHX(7)GG, characteristic of MACPF domains of apicomplexan PLPs (Kafsack and Carruthers, 2010), was used to search all open reading frames (ORF) that coded for proteins with this specific sequence in every available *Babesia* genome (Supplementary Table S1, Brayton et al., 2007; Cornillot et al., 2012; Jackson et al., 2014; Eichenberger et al., 2017; Yamagishi et al., 2017). The presence of a complete MACPF domain, as well as a signal peptide, was analyzed using InterProDomain (https://www.ebi.ac.uk/interpro/). The presence of transmembrane domains was assessed using TMpred (https://embnet.vital-it.ch/software/TMPRED_form.html). The presence of the β-sheet rich domain in the C-terminal end was determined predicting the secondary structure with Jpred4 (http://www.compbio.dundee.ac.uk/jpred/). OrthoMCL tool (https://veupathdb.globusgenomics.org/, Fischer et al., 2011) was used to assign *Babesia* PLP proteins to groups of orthologs present in the database (https://orthomcl.org/orthomcl/, Release 6.1). To evaluate the synteny of the chromosomal regions encompassing PLPs, an alignment of the genomic region containing the target gene in different *Babesia* species was visualized in PiroplasmaDB (https://piroplasmadb.org/, Aurrecoechea et al., 2017) and the conservation and distribution of genes was analyzed. *B. canis* was not included in the synteny analysis since its genome is not available in this database.

2.2 Phylogenetic analysis

Amino acid sequence alignments of the complete PLPs, the MACPF and APC-β domains were conducted with Clustal Omega (Madeira et al., 2019). Phylogenetic analyses were performed with the Maximum Likelihood method using the Kimura 2-parameter model with *T. gondii* PLP1 (GenBank: ABK97634.2) selected as an outgroup. In all cases, bootstrap values were calculated with 1000 replicates. Phylogenetic analyses were done using MEGA version X (Kumar et al., 2018).

2.3 3D structure and function prediction of PLPs

I-TASSER (https://zhanglab.ccmb.med.umich.edu/I-TASSER/, Yang and Zhang, 2015) was used to predict the tertiary structure of PLP proteins from *B. bovis*. Separate structural predictions were done for the complete protein and for the isolated MACPF and APC-β domains. C-scores higher than -1.5 indicate a correct global topology.

After the structure prediction, I-TASSER uses the TM-align structural alignment program to match the obtained model to all structures in the PDB library and COACH to predict possible ligand binding sites. A TM-score takes values between 0 and 1, where 1 indicates a perfect match between two structures and TM-scores higher than 0.5 indicate the same fold.

The visualization and analysis of the modelled structures was performed with UCSF ChimeraX (Goddard et al., 2018).

2.4 Transcription data analysis

Transcriptomic data sets were analyzed to determine the transcription levels of *B. bovis plp* genes in blood stages of two strains of contrasting virulence (Pedroni et al., 2013; http://www.ncbi.nlm.nih.gov/geo/query/acc.cgi?acc=GSE51560) and in two different life cycle stages (kinete-tick and merozoite-bovine) of a virulent strain (Ueti et al., 2020; https://www.ncbi.nlm.nih.gov/geo/query/acc.cgi?acc=GSE144066). The normalized reads from each of the *plp* and housekeeping genes (actin: BBOV_I000300 and fructose-1,6-bisphosphate aldolase: BBOV_IV000790) were analyzed. Gene transcription was considered significantly and differentially regulated if $|\log \text{fold change (FC)}| \geq 1$ and false detection rate (FDR) < 5%.

2.5 Recombinant protein expression and purification

The BboPLP1 MACPF domain (1037 bp) was PCR amplified from genomic DNA (gDNA) of the Argentinean virulent strain S2P using the primers BboPLP1_MACPF Fw: 5'-ACTGATGCCGAAGGAAG-3' and BboPLP1_MACPF Rv: 5'-TCAATCGCGGCGGTACAA-3'. The PCR product was cloned directly into the Gateway

157 entry vector pCR™8/GW/TOPO™ (Invitrogen) and further subcloned in the prokaryotic expression vector
158 Gateway™ pDEST™17 (Invitrogen) in frame with a 6X His-tag in the N-terminal end of the protein. This
159 plasmid was used to transform chemically competent *E. coli* strain BL21 AI™ (Invitrogen) that were further
160 plated in media containing ampicillin. Recombinant BboPLP1_MACPF (rPLP1_MACPF) was expressed by
161 culturing transformed bacteria in LB medium with ampicillin and inducing the culture with 0.2% arabinose
162 for 4 h when O.D. reached 0.4-0.6, at 37°C. Protein expression was confirmed by SDS-PAGE followed by
163 Coomassie Blue staining and immunoblotting using a commercial anti-His antibody (Amersham
164 Biosciences). Purification from inclusion bodies under denaturing conditions was done using a Ni-Agarose
165 resin (Probond™, Invitrogen) as mentioned in Wilkowsky et al., 2011. To obtain soluble rPLP1 MACPF
166 protein for hemolysis assays, expression was induced at O.D. 0.4-0.6 with 0,1% arabinose, at 16°C for 18 h.
167 Soluble recombinant protein was purified as described in Jaramillo Ortiz et al., 2016. The recombinant
168 protein SAG-1 from *Neospora caninum* (rSAG-1) was prepared as previously reported (Wilkowsky et al.,
169 2011).
170
171 *2.6 Antisera Production*
172 Polyclonal immune serum against the rPLP1_MACPF was prepared by immunization of 5 mice with four
173 inoculations, each of 30 µg of protein, at 2-week intervals. First subcutaneous inoculation was emulsified in
174 Freund's complete adjuvant (Sigma Aldrich), followed by three subcutaneous inoculations emulsified in
175 Freund's incomplete adjuvant (Sigma Aldrich). Sera was collected two weeks after the final immunization
176 by exsanguination of mice. Western blot analysis was performed to check specificity and optimal working
177 dilutions (see section below). The care, handling, immunization protocols and euthanasia of animals were
178 performed according to international standards, under guidelines of the Institutional Committee for the
179 Use and Care of Experimentation Animals (CICUAE – INTA protocol N. 42/2016).
180
181 *2.7 Immunoblot*
182 Recombinant PLP1_MACPF protein or *in vitro* culture derived cell lysates of *B. bovis* merozoites of the S2P
183 strain were separated by SDS-PAGE and transferred to a nitrocellulose membrane. For Western blots, the

membrane was incubated with anti-rPLP1_MACPF sera (1:20), anti rRAP-1 sera (1:200), anti-histidine tag antibody (1:3000, Amersham Biosciences), or bovine sera from animals (n=5) naturally infected with *B. bovis* (1:25). For colorimetric detection, secondary antibodies against each species and conjugated to alkaline phosphatase were used (1:10000, Sigma Aldrich). The reaction was developed with BCIP/NBT Color Development Substrate (Promega) as indicated by the manufacturer. For chemiluminescent detection, secondary antibodies conjugated to HRP (1:10000, Abcam) were used and membranes were developed with an enhanced chemiluminescence detection kit (ECL, Pierce™ ECL Western Blotting Substrate, Thermo Scientific) following the manufacturer's procedure.

2.8 Hemolysis assays

The hemolysis assays were carried out as previously described by Garg et al., 2013 with minor modifications. Briefly, to obtain RBC, blood samples from healthy bovines were aseptically collected by jugular venipuncture into a heparinized syringe and centrifuged at 300 × g for 10 min at 4°C. RBC were washed in 9 volumes of PBS three times. Donor animals are regularly housed at the animal facility at Instituto Nacional de Tecnología Agropecuaria under standard animal care protocols (CICUAE – INTA protocol N. 43/2015).

Purified rPLP1_MACPF was incubated at different concentrations with bovine RBC at 2% final hematocrit in a reaction buffer containing 150 mM NaCl, 1 mM $CaCl_2$, 20 mM Hepes (pH 7.2) for 30 min at 37°C. After incubation, cells were pelleted by centrifugation at 900 x g for 10 min. Supernatant was collected and the release of hemoglobin was estimated by measuring absorbance at 405 nm in a 96-well plate spectrophotometric reader and normalized to 1% Triton X-100 as the maximum lysis value. Negative controls were done incubating the washed RBC in the reaction buffer without the addition of proteins or with the addition of the non-lytic rSAG-1 protein.

To evaluate the Ca^{2+} -dependent lysis, the reaction buffer was prepared either with varying concentrations of $CaCl_2$ (0.25, 0.5, 0.75 and 1 mM) or with 1mM EGTA. To evaluate the pH -dependent lysis, RBC were resuspended in PBS of indicated pH (prepared by mixing sodium mono- and diphosphate in different amounts and adjusting pH with 1N HCl or NaOH), as previously described by Roiko et al., 2014. In both

assays, 100 nM of recombinant protein were used, and for the pH -dependent lysis assay additional negative controls were included, in which washed RBC were incubated in PBS of different pH (5, 7 and 9) to verify that the effect observed was due to changes in protein activity at different pH rather than by changes of pH itself.

The assays were performed in triplicate and to evaluate the statistical significance of the results, a one-way ANOVA test was performed, followed by a Dunnett test of multiple comparisons. $p < 0.001$ was considered significant. Statistical analysis was done using GraphPad Prism version 5.01 for Windows, GraphPad Software, La Jolla California USA, www.graphpad.com.

2.9 In vitro culture of B. bovis

The *B. bovis* S74-T3Bo parental strain and the knock out line generated in this work were cultured in long-term microaerophilic stationary phase culture using 10% of bovine RBC in HL-1 medium supplemented with bovine serum as previously described (Levy and Ristic, 1980; Rodriguez et al., 1983). Both strains are maintained as a cryopreserved stabilates in liquid nitrogen when not in use (Palmer et al., 1982).

2.10 Construction of the transfection plasmid pBboΔplp1

The transfection plasmid p6-Cys-EKO containing the fluorescent protein eGFP fused to Blasticidin-S deaminase (BSD) under the control of the ef-1α promoter described by Alzan et al., 2017, was used as a backbone to construct the pBbo*Δplp1* plasmid for stable transfection (Supplementary Fig. S1). The 5' untranslated region (UTR) and 3' UTR of the *plp1* gene were PCR amplified from gDNA of *B. bovis* S74-T3Bo strain and cloned into the *XhoI* and *BamHI* sites of the plasmid, respectively. The 5' UTR fragment was amplified by PCR using primers 5'UTR-PLP1-F-*XhoI* 5'-GCGTGCCTCGAGAAAACCGCTTGTGTTTAACG-3' and 5'UTR-PLP1-R-*XhoI* 5'-GCGTGCCTCGAGTGCGATAATAAGTGAAATGTGTC-3'. The 3' UTR was amplified using primers 3'UTR-PLP1-F-*BamHI* 5'-CGCTATGGATCCCAGACATGGTACCCCTGTAAC-3' and 3'UTR-PLP1-R-*BamHI* 5'-CGCTATGGATCCCTACCAGTAAGTAATCGGTTGTTTT-3'. After PCR, amplicons were purified and cloned into pGEM®-T easy vector (Promega) followed by sequential subcloning in the transfection plasmid p6-Cys-EKO by digestion with either *XhoI* or *BamHI.* Restriction digestion of p6-Cys-EKO with these enzymes results in

238 the removal of the 6-Cys-E fragments which were replaced with the *plp1* UTR fragments. The resulting
239 transfection plasmid, named pBbo*Δplp1*, was sequenced in both strands using T7 promoter and T3
240 promoter primers, at the sequencing facility of IABIMO, INTA-CONICET, Argentina.
241 Prior to *B. bovis* transfection, One Shot™ TOP10 Chemically Competent *E. coli* (Invitrogen) were
242 transformed with the pBbo*Δplp1* plasmid which was subsequently purified with Qiagen Plasmid MidiKit
243 (Qiagen) following the manufacturer's instructions. Control plasmid pBluescript was purified identically and
244 used as a control in transfection experiments.
245
246 *2.11 Transfection of B. bovis*
247 The plasmid pBbo*Δplp1* was electroporated into *B. bovis* S74-T3Bo strain as previously described (Suarez et
248 al., 2006; Suarez and McElwain, 2009). As a negative control of the transfection experiment, parasites were
249 electroporated with an empty pBluescript plasmid in identical conditions. After transfection, parasite
250 cultures were transferred to an incubator at 37°C. After 12 h, an inhibitory concentration of blasticidin was
251 added to the media for selection of transfectants. Cultures were monitored daily for the presence of
252 transfected fluorescent parasites with a fluorescence microscope (Zeiss) at 60X magnification. After eGFP
253 fluorescent parasites emerged, cultures were grown for additional 30 days (15 passages) in the presence of
254 inhibitory concentrations of blasticidin before being submitted for genetic analysis.
255
256 *2.12 Genetic characterization of the B. bovis Δplp1 strain by PCR and sequencing*
257 To verify the integration and disruption of the *plp1* gene in the knockout strain, different PCR assays were
258 performed on gDNA from the wild type (WT) strain S74-T3Bo, the *Δplp1* strain and pBluescript transfected
259 parasites using primers listed in Supplementary Table S2. A schematic representation of the construct and
260 primer hybridization sites is shown in Supplementary Fig. S2. A PCR targeting the *msa1* locus was also
261 performed in all cases to evaluate the integrity of the gDNA. All amplicons were cloned into TOPO® TA
262 Cloning vector (Invitrogen) and sequenced using plasmid primers.
263
264 *2.13 Enrichment of transfected cultures*

After transfection and selection with antibiotic, the parasite culture was subjected to fluorescence-activated cell sorting using SY3200 FACS (Sony Biotechnology) to obtain a clonal line of *Δplp1* eGFP-expressing parasites. To this end, 500 eGFP-positive and infected RBC were collected and used to start new cultures. Fluorescence microscopy and flow cytometry analysis were performed on the original and the enriched cultures to confirm that the latter did not contain detectable non-fluorescent WT parasites.
For the microscopy analysis, the original and the enriched cultures were stained with Hoechst 33342 (Thermo Scientific) to identify the parasite nucleus. Samples were visualized using Leica DMi8 inverted microscope with bright field, ultraviolet fluorescence and 100X magnification. Images were processed using Leica LAS X analysis software to produce individual and merged images.
Flow cytometry assays were conducted using a Millipore Guava easyCyte HT flow cytometer. Samples from the enriched *Δplp1* and WT cultures were analyzed, as well as artificial mixtures of 1:1 and 10:1 (*Δplp1*:WT) that were used as controls. All samples had been previously stained with hydroethidine (Dihydroethidium Invitrogen) to confirm the presence of the parasite. Measures of hydroethidine and eGFP were registered for all analyzed samples.

2.14 Growth curve assay

To identify the possible impact of the *plp1* deletion on the growth of *B. bovis*, the ability of *Δplp1* parasites to replicate in *in vitro* cultures was evaluated and compared to the WT. Cultures of each strain were initiated at 0.5% parasitemia in triplicate wells. Culture medium was replaced every 24 hs and the parasitemia was calculated daily for 4 days. Statistical analysis was performed with the Student's t-test, and the probability value of less than 5% ($p < 0.05$) was considered significant.

2.15 RNA extraction and complementary DNA synthesis

For the generation of cDNA, *in vitro B. bovis* cultures of either the enriched *Δplp1* or the WT strains with 13 and 5.6 percentage of parasitized erythrocytes (PPE), respectively, were used for RNA isolation using Trizol solution (Ambion, Life Technologies). Cultures were centrifuged and the pellets were resuspended in 3 volumes of Trizol. Total RNA was isolated as indicated by the manufacturer, resuspended in 25 µl of

diethylpyrocarbonate-treated water and treated with Turbo DNA free-DNase (Ambion, Life Technologies). Reverse transcriptase-polymerase chain reaction (RT-PCR) was carried out for cDNA synthesis using the SuperScript™ First-Strand Synthesis System for RT-PCR (Invitrogen) with random hexamer primers (Thermo Scientific) using current protocols.

2.16 Quantitative PCR (qPCR) of plp1

qPCR of *hsp20* (BBOV_II004080) and *plp1* genes were carried out using the primers hsp20_qF: GAACCCGATTACTTTCAACCCA; hsp20_qR: TGTCAGTGCTGCTGAAACCAG; plp1_qF: GTTGACCCAGGATACAGGCATC; plp1_qR: GATCCATCCACCCTTAGGCTCT. These primer pairs amplify fragments of approximately 150 bp. qPCR reactions were done using SsoAdvanced Universal SYBR Green Supermix (Biorad) in a final volume of 15 µl with 50 nM of each specific primer and 100 ng of cDNA. The cycling parameters consisted of 1 cycle at 98 °C for 10 min and 40 cycles of 98 °C for 10 s followed by 62 °C for 60 s. At the end of the cycle, a standard melting curve was performed to verify the specificity of the generated amplicons. Quantifications were done with the relative standard curve method using the StepOne™ v2.3 software. The *hsp20* gene was used as endogenous control and the cDNA from the WT strain as reference. In all the cases, three replicates per strain were used.

3. Results

3.1 Identification of members of the perforin-like proteins gene family in Babesia

Previous work defined a signature motif of 20 conserved amino acids present in the MACPF domain of PLP proteins of several apicomplexan parasites (Kafsack and Carruthers, 2010). We used this motif to search the genomes of 11 *Babesia* species and strains (Supplementary Table S1) for ORFs containing this MACPF motif. Full conservation of the MACPF domain (ranging from 118 to 232 amino acids) was confirmed in the 38 *Babesia* ORFs identified, according to the InterProDomain database. In addition, signal peptides were detected in 60% of the predicted proteins.

As expected, PLP coding genes were identified in all the examined *Babesia* genomes and the number of genes varied between the species. In the case of *B. bovis, B. ovata* and *B. microti*, six hypothetical PLPs

were found. In *B. bovis* and *B. microti* one of these proteins, PLP3, contained three putative MACPF domains within a single ORF. In *B. bigemina* and *B. divergens*, a total of eight PLPs were identified, each one containing only one MACPF domain. A smaller number of members of the PLP family was found in *B. canis,* with only four *plp* genes, also with only one MACPF domain.

Moreover, the characteristic APC-β domain was found in PLP proteins of all *Babesia* species, except for *B. canis* in which none of the proteins contained this domain. In particular, this β sheet-rich domain was present in every PLP1, PLP6 and PLP7, while this domain was not found in any PLP2 or PLP8. In the case of PLP3, the APC-β domain is absent in all species except for *B. bovis* in which it is located between MACPF domains 2 and 3 and not in the C-terminal end of the protein. The APC-β domain in PLP4 is absent only in the *B. bovis* ortholog, and in the case of PLP5, this domain is present in all proteins except for the *B. microti* ortholog. Table 1 summarizes the relevant information on all the identified PLP proteins.

Another four MACPF-containing proteins were identified in *B. ovata*, *B. bovis*, *B. bigemina* and *B. divergens* by a search in PiroplasmaDB (Supplementary Table S3). However, these proteins neither contain the canonical string of amino acids of the MACPF motif of the PLP family nor the APC-β domain in the C-terminal end. Moreover, their respective gene loci showed no synteny with any PLP coding gene. Based on these findings, we assume that these proteins are not canonical perforin-like proteins. Whether this is the result of miss annotation or an evidence of the existence of such non-canonical PLP or non-PLP related proteins with MACPF domains in *Babesia,* deserves further confirmation.

Amino acid conservation of the identified *Babesia* PLPs was evaluated between all analyzed species. When possible, conservation of protein sequence between strains and between orthologs in related apicomplexan parasites was also analyzed. Multiple sequence alignments showed that conservation is limited to the 20 amino acids that comprise the MACPF motif and to the 4 cysteine residues of each tandem repeat of the APC-β domain, where present (Figure 1 and Supplementary Fig. S3 to S5). The amino acid sequence of each PLP is 100% conserved among two otherwise distinct strains of *B. bovis* and *B. divergens*, while minimum differences (evolutionary distances ranging from 0.01 to 0.03) were observed for *B. bigemina* strains (n=4). In all cases these amino acid substitutions were between residues of same physicochemical characteristics (data not shown).

A phylogenetic tree was constructed based on the MACPF domain of *Babesia* PLPs showing that the MACPF domain of each PLP is conserved among the different species of *Babesia*, maintaining a greater amino acid identity between orthologous proteins than between paralogs (Figure 2). The phylogenetic tree also shows that the first MACPF domain of the *B. bovis* PLP3 protein, named PLP3.1, groups with the PLP3 protein of the other four species, meanwhile the second and third domains of *B. bovis* PLP3 (PLP3.2 and PLP3.3) group with PLP7 and PLP8 of the remaining species, respectively. When the tree was constructed with the amino acid sequences of the complete PLP proteins, greater differences were observed, yet the topology of the tree remained unaltered (data not shown). The parasite *B. microti* was not included in this analysis since it is a *sensu lato Babesia* that belongs to the archaeopiroplasmids, an early branching lineage which is distant from the *Babesia sensu stricto* group (Criado-Fornelio et al., 2003; Schreeg et al., 2016).

To evaluate orthology, each *Babesia* PLP was assigned to one of the groups defined in the OrthoMCL database (Supplementary Table S4). The 38 proteins were assigned to 8 different groups. In particular, group OG6_121849 contains not only PLPs from *Babesia* spp. but also previously characterized PLP proteins from *Plasmodium* and *Toxoplasma*.

Additionally, synteny of the chromosomal regions containing *plp* genes was evaluated. The analysis showed that the identity and order of genes surrounding *plp*s is highly conserved among the *Babesia* species analyzed here (Supplementary Fig. S6). As mentioned before, *B. bovis* and *B. microti plp3* contain three MACPF domains within the same coding sequence, each having high sequence identity with the domains of PLP3, PLP7 and PLP8 of the remaining species. By comparing the genomic organization of these genes in the different species, it is observed that *plp3*, *plp7* and *plp8* are adjacent in *B. bigemina*, *B. divergens* and *B. ovata.* In addition, the respective upstream and downstream genes are syntenic between all the five species.

3.2 Prediction of the three-dimensional structure of the PLP proteins

The majority of the hereby identified *Babesia* proteins show the expected domain architecture for apicomplexan PLPs that include a N-terminal signal peptide, a central canonical MACPF domain and the C-

terminal APC-β domain, formed by three direct repeats, each containing four conserved cysteine residues (Figure 3a).

The 3D structure predictions of BboPLP1 are shown in Figure 3b-d (all *B. bovis* proteins presented similar results, Supplementary Fig. S7). The structure prediction either of the whole protein (Figure 3b) or of the isolated MACPF and APC-β domains (Figure 3c) strongly suggests that, at least for *B. bovis*, all PLPs have the basic structural characteristics of pore forming proteins. More specifically, the predicted structure of the MACPF domain (Figure 3c, left) includes the antiparallel chains (yellow) that form the twisted β-sheet, as well as the two clusters of α-helices (CH1 and CH2, pink) with alternating hydrophobic and hydrophilic amino acids that are typical features of these class of domains. The predicted 3D structure of the APC-β domain (Figure 3c, right) evidences a single globular domain with 4 highly conserved cysteine residues in each repetition, that are located in opposite positions allowing the formation of disulfide bonds between them, helping stabilize the structure (Figure 3d and e). Furthermore, a possible Ca^{2+} binding site mediated by amino acids G866 and E868 was predicted in this domain (Figure 1, blue arrows).

When the predicted structures were compared to other protein structures deposited in PDB, striking similarities with other well characterized pore forming proteins were observed (Supplementary Fig. S8). In particular, the closest structure to the complete BboPLP1 protein was the human complement component C6 (PDB: 3t5o, TM-Score: 0.756), while the isolated MACPF domain was most similar to the lymphocyte perforin (PDB: 3nsj, TM-Score: 0.811). As for the APC-β domain, high structural concordance with the APC-β domain of TgPLP1 (PDB: 6d7a, TM-Score: 0.968) was observed. Overall, structural analysis indicates that conservation of three-dimensional structural features of the members of the PLP family despite the occurrence of considerable sequence diversity among the PLP proteins is necessary to fulfill functional requirements during the life cycle of the parasites.

3.3 Differential expression of PLPs throughout B. bovis live stages

A profile for the pattern of transcription of the *B. bovis plp* genes in erythrocytic (virulent and attenuated strains) and tick stage parasites was obtained upon analysis of global transcriptomic data sets generated previously (Pedroni et al., 2013; Ueti et al., 2020). Dataset analysis revealed that all *plp* genes are expressed

by these parasites during life cycle stages that occur in the vertebrate host or in the tick vector. Interestingly, comparative analysis shows that some genes are differentially transcribed between the two analyzed stages. More specifically, the *plp1* and *plp5* genes are mostly transcribed in merozoites, while *plp2* shows the highest levels of transcription in kinetes (Figure 4a). On the other hand, the transcriptomic data set of merozoites from a virulent and its attenuated derivative strain, not only confirmed the stage specific expression of *plp1* but also revealed a different rate of transcription being 1.8 times higher in the virulent strain compared to its attenuated counterpart (Figure 4b). Thus, transcriptional analysis revealed differential expression of the members of the PLP family among distinct stages and virulence phenotypes, suggesting they may play relevant functional roles during life stage transitions and virulence.

3.4 Functional characterization of B. bovis PLP1

To deepen the study of *Babesia* PLPs we focused on *B. bovis* proteins since this species causes the most severe clinical scenario in infected bovines. We selected for the functional characterization the *B. bovis* PLP1 (BboPLP1) protein based on several factors. First, BboPLP1 belongs to the OG6_121849 orthology group that also contains previously characterized PLPs from *Plasmodium* and *Toxoplasma* which have been proven to be essential for the virulence of these pathogens. Second, the overall tertiary structure of BboPLP1 has a high degree of similarity with other pore-forming proteins, showing all the elements necessary for pore formation. Finally, *plp1* gene transcription is higher in blood stage and virulent parasites, which are directly associated with the clinical signs of the disease, suggesting that PLP1 may be a virulence factor.

The recombinant MACPF domain of BboPLP1 (rPLP1_MACPF; 42,4 kDa) was expressed in *E. coli* and used to generate polyclonal antisera that weakly reacted with a protein which size is compatible with the full size of the PLP1 protein (108 kDa) in lysates of *B. bovis* merozoites (Supplementary Fig. S9a). Importantly, antibodies present in a set of sera from *B. bovis* infected bovines were able to react with rPLP1_MACPF (Supplementary Fig. S9b), representing the functional domain of PLP1, suggesting that this region contains B-cell epitopes recognized during infection.

To evaluate if PLP1 has membranolytic activity that can be associated to the MACPF domain, the purified rPLP1_MACPF protein was incubated with bovine RBC in different conditions to test for hemoglobin release. rPLP1_MACPF protein was capable of generating damage in the membranes of RBC reaching hemolysis levels of 90%, compared to the treatment with 1% Triton X-100 (Figure 5a). In contrast, the non-related protein SAG-1 of *Neospora caninum* used as negative control did not have any hemolytic effect.

We then evaluated whether rPLP1_MACPF is able to lyse bovine erythrocytes in a dose-dependent fashion. A dose-response curve was performed with protein concentrations in a range of 30 to 250 nM (Figure 5b). Results showed that when concentrations are lower than 75 nM, the hemolysis values are below 10%, while surpassing this concentration generates an abrupt increase in hemolysis, reaching values of more than 90% when concentration is above 90 nM of protein. This suggests that a critical concentration of the recombinant protein is required in order to effectively function as a hemolysin.

In addition, we investigated the effect of pH on the hemolytic activity. The highest levels of hemolysis were observed in the range of pH 5.5 to 9 (Figure 5c). Finally, hemolysis at different Ca^{2+} concentrations was also evaluated and although maximum activity was observed at Ca^{2+} concentrations around 0.5 mM, there were no large differences in hemolysis in the presence or absence of the ion (Figure 5d). Therefore, our data indicates that PLP1 has hemolytic activity *per se*, which can be associated with the region of the protein that includes the MACPF domain.

3.5 A B. bovis plp1 knockout line is less fit than the wild type parental line when developing in in vitro *cultures*

A *plp1* knock out (*Δplp1*), was generated by transfection of *B. bovis* with plasmid pBbo*Δplp1*, and blasticidin-resistant and eGFP fluorescent parasites emerged 5 days after addition of the antibiotic. No parasites were detected in the culture transfected with the pBluescript empty plasmid after five days of selection with blasticidin (Figure 6).

Specific integration of the *egfp-bds* cassette disrupting the *plp1* locus by homologous recombination was evaluated by PCR combining different primer sets (Supplementary Fig. S2) followed by sequencing of the respective amplicons. Figure 7 shows results obtained for PCRs I and III which target the 5' and 3' insertion

sites of the *egfp-bds* cassette in the *plp1* locus, respectively. Equivalent results were obtained for PCRs II and IV (data not shown). More specifically, the size and sequence of the PCR products obtained with PCR I and II were fully consistent with the disruption of the *plp1* gene by insertion of the *egfp-bds* selection marker. Surprisingly, positive PCR amplification was also obtained for the control PCR III and IV in two cultures of Δ*plp1* strain from two independent transfections, suggesting that the cultures contained a mixed population of WT and Δ*plp1* parasites.

In view of these findings, we generated the enriched line of *B. bovis Δplp1* (e*Δplp1*) from the mixed *Δplp1* strain. The success of the enrichment was first evaluated through fluorescence microscopy observation (Figure 8). The images demonstrated that, in contrast to the *Δplp1* mixed population, all parasites in the enriched *Δplp1* culture express eGFP, a result that was further confirmed by flow cytometry assays (Figure 9). In addition, evaluation of transcription of the *plp1* gene in the e*Δplp1* line demonstrated the absence of transcripts of the knock out gene indicating the purity of the parasite line (Supplementary Fig. S10).

The enriched line of *B. bovis Δplp1* was used to evaluate the possible contribution of *plp1* on the proliferative capacity of the parasite and the rate of *in vitro* growth upon comparison with the wild type S74-T3Bo strain. Significant differences ($p < 0.05$) were found in the *in vitro* growth rate at days 2 and 4 among these parasite lines (Figure 10a), suggesting that the parasites in the enriched line of *B. bovis Δplp1* are less fit than the wild type parasites to grow in the *in vitro* culture system. In addition, a striking feature that appeared in the stained smears of the e*Δplp1* line analyzed under the light microscope was the presence of uncommon structures consisting of more than a pair of merozoites inside the RBC (Figure 10b). These abnormal structures appeared at a frequency of ≈8% of infected RBC. Thus, significant phenotypic features are altered in *plp1* deficient blood stage parasites, strongly suggesting that expression of *plp1* is required for optimal fitness of the parasite during its development on the bovine host.

4. Discussion

The egress mechanism of apicomplexan parasites has been understudied and is of special interest to better understand host-pathogen interaction. Perforin-like proteins have been unequivocally assigned to have a key role in egress and cell transversal in medically relevant *Apicomplexa*. Several reports describe the

presence of genes coding for PLP proteins in *Babesia* (de Vries et al., 2006; Brayton et al., 2007; Kafsack and Carruthers, 2010; Wade and Tweten, 2015; Moreno-Hagelsieb et al., 2017; Elton et al., 2019; González et al., 2019). However, no functional characterization of any member in this genus has been done so far.

In this work, genomic analysis using different bioinformatic tools allowed us to identify and characterize the complete PLP protein family in different *Babesia* species. Comparative analyses show that conservation is limited to the secondary and tertiary structure of the proteins. Meanwhile, primary sequence conservation is restricted to the 20 amino acids that comprise the $MACPF^{api}$ motif already described (Kafsack and Carruthers, 2010) and to the cysteine residues of the APC-β domain when this domain is present (Guerra et al., 2018; Ni et al., 2018). Our analyses also show greater amino acid identity between orthologs than between paralogs, a feature also observed for *Plasmodium* PLPs (Kaiser et al., 2004), suggesting that each member of the PLP family may have evolved independently to play different functional roles.

Babesia genomes code for a relatively large number of *plp* genes (6 to 8 depending on the species), except for *B. canis* where only 4 *plp* genes were found. We attribute this to the fragmentation of *B. canis* genome in a large number of scaffolds (Eichenberger et al., 2017). It has been reported that incorrect genome assemblies result in inferring a wrong number of genes belonging to a gene family (Denton et al., 2014), so the number of *plp* genes in *B. canis* should be revised. Genomes of *Plasmodium* also code for a large family of *plp* genes, whereas coccidian parasites such as *T. gondii* or *N. caninum*, only have one or two *plp* genes.

Our analysis on *Babesia* PLPs support the hypothesis proposed by Kafsack and Carruthers in 2010 that argues that the expansion of the PLPs family might have been originated by the need to adapt PLP functions to both their mammalian and arthropod hosts when apicomplexans evolved from a monoxenic to a dixenic life cycle as in Hematozoa. Interestingly, transcriptomic data of the kinete (tick) and blood (mammal) stages show that even though all genes are transcribed throughout the parasite´s life cycle, most of them have variable stage specific transcription levels, providing more support to the hypothesis mentioned above.

Regarding the architecture of *Babesia* PLP proteins, a signal peptide was bioinformatically detected in 60% of them suggesting that they are either secreted or reside in the lumen of organelles. The lack of this peptide in some of *Babesia* PLPs is likely due to the difficulty in predicting the start of the first exon of the

gene or to the fact that the prediction algorithms are trained with prokaryotic organisms and with a limited number of eukaryotes. Based on previous information of other apicomplexan PLPs (Kadota et al., 2004; Kaiser et al., 2004; Ishino et al., 2005; Kafsack et al., 2009; Garg et al., 2013), these proteins are expected to be stored at micronemes prior to being secreted. So far, PLP4 of *P. berghei* is the only exception since it is located in vesicles different from micronemes, in the apical end of the parasite (Deligianni et al., 2018). Most of the PLPs already described in *Apicomplexa* have only one pore forming domain per protein. The *in silico* prediction of the tertiary structure of the MACPF domain for *B. bovis* PLPs showed the presence of characteristic α-helix clusters surrounding antiparallel chains that form the β-sheet which play a key role in the formation of the pore. Interestingly, it has been previously reported that PLP3 of *B. bovis* and PLP5 of *T. annulata* have three MACPF domains within a single ORF (Kafsack and Carruthers, 2010). In this work, we confirmed that PLP3 has multiple domains in the two *B. bovis* strains analyzed and also in its ortholog in *B. microti*. We also show that each of the MACPF domains of PLP3 from *B. bovis* and *B. microti* has high sequence identity with the equivalent domains of PLP3, PLP7 and PLP8 of the other *Babesia* species. Moreover, when comparing the genomic organization of these genes in the different *Babesia* species, we observed that *plp3*, *plp7* and *plp8* are adjacent in *B. bigemina*, *B. divergens* and *B. ovata* with the upstream and downstream genes conserved between all the analyzed species. Finally, analyzing the presence and position of the APC-β domain in these particular PLPs we observed that neither PLP3 nor PLP8 of *B. bigemina*, *B. divergens* and *B. ovata* have this C-terminal domain while PLP7 does, and that the multidomain PLP3 of *B. bovis* has only one APC-β domain between the second and third MACPF domains. Based on these observations, we hypothesize that the *B. bovis* and *B. microti plp3* gene might have emerged as a fusion of adjacent genes.

According to the pore forming mechanism proposed by Baran et al., 2009 for the lymphocyte perforin, MACPF proteins are secreted as monomers that, after binding to the target membrane, oligomerize forming large ring complexes that undergo a marked structural reorganization creating the pore. Assuming this model, the increase in the number of MACPF domains within a single protein would minimize the number of identical monomers required to form the pore, a characteristic that would have been positively selected since the compaction of genomes in obligate parasites was a frequent event throughout evolution

(Templeton et al., 2004; Lawrence, 2005; Kuo and Kissinger, 2008; Cornillot et al., 2012). We speculate that this would be the case of *B. bovis* and *B. microti* where the pore would combine monomers of the PLP3 protein. However, in the case of the rest of *Babesia* species and according to our phylogenetic analysis, the pore would form in a similar fashion to complement proteins involving monomers of PLP3, PLP7 and PLP8. This hypothesis is supported by our phylogenetic analysis that showed that putative PLP3 MACPF domains 3.1, 3.2 and 3.3 of *B. bovis* and *B. microti* group with PLP3, PLP7 and PLP8 of the other species.

In addition to the MACPF domain, the APC-β domain containing the four conserved cysteine residues in the tandem repeats that is characteristic of apicomplexan PLPs was also identified in the C-terminal region of most *Babesia* proteins. The position of these cysteines is compatible with the formation of disulfide bonds between them, a structure that is highly conserved with that of the APC-β domain of *T. gondii* PLP1 (Guerra et al., 2018; Ni et al., 2018). The absence of the APC-β in some *Babesia* PLPs suggests that these proteins may interact with a second protein that could modulate its activity (Kafsack and Carruthers, 2010).

It is important to note that the predicted APC-β domain structures were different when modelled as part of the complete protein or isolated from the other domains. The model of the complete protein was based on the human complement component C6 and the APC-β domain is unique to apicomplexan parasites. Conversely, the APC-β domain was modeled based on the equivalent domain of *T. gondii* PLP1 and therefore likely constitutes a more accurate prediction of the structure of the APC-β domain. Despite being less rigorous, the predicted structure of the complete proteins provides insights on the overall structure of PLPs and how it resembles that of other pore forming proteins, with a central MACPF domain and a salient C-terminal domain.

The marked structural conservation of *Babesia* PLPs with other pore forming proteins, on the face of otherwise massive sequence polymorphisms, demonstrates an evolutionary restriction to variation and supports our hypothesis that *Babesia* PLPs are related to pore formation. To test this hypothesis, we selected the PLP1 protein of *B. bovis* to continue with the functional characterization since it is the PLP with the highest transcription levels in *B. bovis* blood stage parasites. Besides, the evidence of PLP1 orthologs in *Plasmodium* (PPLP1 and PPLP3) (Kadota et al., 2004; Kaiser et al., 2004; Ishino et al., 2005; Amino et al., 2008; Garg et al., 2013; Risco-Castillo et al., 2015) and *Toxoplasma gondii* (TgPLP1) (Kafsack et al., 2009;

560 Roiko and Carruthers, 2013) has shown that these proteins play important and well defined roles in the
561 parasite´s virulence.
562 Western blot analysis showed that sera from *B. bovis* infected bovines have antibodies against the
563 recombinant MACPF domain of PLP1 confirming that PLP1 is expressed by merozoites and contains B-cell
564 epitopes that are exposed to the host immune system during infection. However, the fact that these
565 animals are persistently infected with *B. bovis* indicates that the anti MACPF antibodies do not prevent the
566 parasite´s invasion of RBC and support our hypothesis that PLP1 has a predominant role in egression
567 instead. Another explanation to this observation is that the role of PLP1 on parasite invasion would be
568 redundant.
569 We have also demonstrated that polyclonal antisera against rPLP1_MACPF recognized the complete native
570 PLP1 protein, indicating conservation of B-cell epitopes in the recombinant protein. The low signal in PLP1
571 detection may imply that this protein is expressed in low amounts in the parasite.
572 It is remarkable that the MACPF domain of PLP1 is sufficient for pore formation since it is capable of lysing
573 RBCs, even is when it lacks the context provided by the rest of the protein. It is possible however, that the
574 tertiary structure and context provided by the full PLP1 protein is required for regulation of the pore
575 forming activity of PLP1 which likely requires strict control in terms of specificity and timing. Another aspect
576 to highlight is that PLP1 showed hemolytic capacity in the opposite direction to that expected for a protein
577 that is secreted from the parasite to the RBC cytoplasm. This is in agreement with previous studies done on
578 *T. gondii* PLP1 which is involved in the parasitophorous vacuole membrane rupture prior to egress, and yet
579 showed cell lysis activity on both the luminal and cytoplasmic sides of the parasitophorous vacuole
580 membrane (Kafsack et al., 2009). Furthermore, studies done on *Plasmodium* PLP1 and PLP2 that are
581 involved in the egress of the parasite from the RBC also showed this reversible hemolytic capacity (Garg et
582 al., 2013; Wirth et al., 2014). The molecular mechanisms of PLP1 mediated lysis remain undefined, but it
583 may be possible to speculate that the receptor(s) required for mediating lysis by PLP1 are expressed at both
584 sides of the erythrocyte membrane.
585 Low concentrations of rPLP1_MACPF do not generate hemolysis, while surpassing a threshold
586 concentration generates maximum levels of RBC damage which is in agreement with the model of Baran et

al., 2009. This positive-cooperative response suggests that a critical amount of protein is needed in the membrane before the pore can be formed resulting in subsequent hemolysis. Interestingly, the same findings were reported for the functional domain of PfPLP1 (Garg et al., 2013) and for the lymphocyte perforin, a non-apicomplexan pore forming protein (Voskoboinik et al., 2005; Dong et al., 2007; Baran et al., 2009), and are consistent with the proposed mechanism for pore formation previously mentioned.

The rPLP1_MACPF domain showed high levels of hemolysis in a wide pH range including the pH≈7 within the RBC and in plasma, and a drop of protein activity was observed at pH below 5.5. The predicted isoelectric point of the recombinant protein is around 5.6 and therefore it is likely that the drop in hemolysis levels observed at pH below 5.5 is caused by protein aggregation and precipitation, leaving the protein inactive.

Furthermore, we evaluated hemolysis in different calcium concentrations since it has been reported that egress of *B. bovis* from RBC is Ca^{2+} dependent (Mossaad et al., 2015). We observed no differences in hemolysis in the presence or absence of the ion, which is in agreement with previous reports on PfPLP1 (Garg et al., 2013) where although the activity of the complete protein is Ca^{2+} sensitive, the hemolytic capacity of the isolated MACPF domain does not change in response to this ion. In this sense, the modeling of the APC-β domain of BboPLP1 performed in this work predicts a possible Ca^{2+} binding site in the C-terminal region of the protein. This observation suggests that PLP1 has an independent calcium binding domain outside from the MACPF that may modulate its activity. Previous works on the lymphocyte perforin (Voskoboinik et al., 2005) and on PfPLP1 (Garg et al., 2013, 2015) showed that the C-terminal region of both pore forming proteins are responsible for the Ca^{2+}-dependent membranolytic activity. These evidences allow us to hypothesize that, like its ortholog in *P. falciparum*, *B. bovis* PLP1 has a Ca^{2+} binding site located outside the MACPF domain, presumably in the APC-β domain, that plays a role regulating the hemolytic activity of the MACPF domain. These results altogether suggest that the APC-β domain in Hematozoa might play a different role than the APC-β domain of *T. gondii* PLP1 (Roiko and Carruthers, 2013; Guerra and Carruthers, 2017). Those *Babesia* PLPs that do not have the APC-β domain might be involved in a different mechanism that is not regulated by Ca^{2+} or its activity might be regulated by another Ca^{2+} -sensing protein.

Finally, to evaluate the role of PLP1 in the parasite's life cycle, a *plp1* knock out strain was generated. The *Δplp1* strain was capable of multiplying and growing in *in vitro* RBC cultures showing that PLP1 is not essential for development of parasite's erythrocyte stages. However, we observed that *Δplp1* parasites grow significantly slower than the WT. This decrease in the replication capacity allows us to conclude that the absence of *plp1* negatively affects the proliferation of the erythrocyte stages of *B. bovis*. Interestingly, a low percentage of unusual tetrameric forms in the same RBC were observed in the *Δplp1* parasites. In most *Babesia* species including *B. bovis*, parasites undergo a single cycle of asexual reproduction within the RBC prior to egress, therefore tetrameric forms are not expected (Potgieter and Els, 1977; Mehlhorn and Schein, 1985; Kawai et al., 1986, 1999). A phenotype of similar characteristics was reported in the knockout of *T. gondii* for the orthologous gene *plp1* (Kafsack et al., 2009; Roiko and Carruthers, 2013) in which the *Δplp1* parasites survive in culture at a lower growth rate and with a greater number of parasites within an infected cell. The authors assume that due to the lack of the PLP1, knock out parasites lost their ability to actively egress and continue to replicate inside the same cell for more cycles than usual.

Here, we propose that once mature merozoites are ready to egress, PLP1 is released from the micronemes and binds to the RBC membrane where it oligomerizes forming pores in the membranes facilitating the egress of the parasite. When PLP1 is absent, the merozoite fails to egress efficiently from the RBC after cell division and undergoes a second round of replication within the same cell, generating the tetrameric forms observed. Clearly, PLP1 activity for cell egress is dispensable and its function can be replaced by other proteins, probably other members of the family. Further experiments will be carried out in order to determine whether the PLP1 mutant line has a distinct pattern for the expression of other members of the PLP family.

The mechanism by which these pores give rise to the parasite's egress remains unknown, but one possibility is that the pores change the membrane's permeability generating an osmotic lysis of the erythrocyte, which is consistent with the video-microscopies that show that bovine RBC infected with *B. bovis* bursts prior to the release of merozoites (Asada et al., 2012).

639 Further *in vivo* studies with the *Δplp1* strain will allow us to analyze if the *in vitro* replication defect impedes
640 infection of the vertebrate host or if it results in an attenuated phenotype *in vivo*. Attenuated *Babesia*
641 knock out strains arise as a novel alternative to traditional live vaccines since they cause a mild disease that
642 allows immunization of cattle while remaining genetically stable (Florin-Christensen et al., 2014; Suarez et
643 al., 2017). This would eliminate the risk of phenotypic reversal plus the advantage of allowing
644 discrimination between vaccinated and naturally infected animals (Florin-Christensen et al., 2014). In
645 addition, the effect of the lack of *plp1* on transmission through the vector should be tested since PLP1
646 might also be required for development of tick stages.
647
648 **Acknowledgements**
649 This work was supported by Instituto Nacional de Tecnología Agropecuaria (INTA), Consejo Nacional de
650 Investigaciones Científicas y Técnicas (CONICET), the United States Department of Agriculture-Agriculture
651 Research Service - Current Research Information System Project No. 2090-32000-039-00D and by the USDA
652 National Institute of Food and Agriculture (Award Number: 2020-67015-31809; Proposal Number: 2019-
653 05375, Accession Number: 1022541).
654 We wish to acknowledge Paul Lacy for his outstanding technical support. Also, a fellowship to M.S.P. by the
655 Fulbright Program together with the Bunge y Born and Williams Foundations is gratefully acknowledged.
656 We thank Reginaldo Bastos for his valuable assistance in flow cytometry analysis.
657
658 **Declarations of interest:** none.
659
660 **References**
661 Alzan, H.F., Silva, M.G., Davis, W.C., Herndon, D.R., Schneider, D.A., Suarez, C.E., 2017. Geno- and
662 phenotypic characteristics of a transfected *Babesia bovis* 6-Cys-E knockout clonal line. Parasit. Vectors
663 10, 214. doi:10.1186/s13071-017-2143-3
664 Amino, R., Giovannini, D., Thiberge, S., Gueirard, P., Boisson, B., Dubremetz, J.F., Prévost, M.C., Ishino, T.,
665 Yuda, M., Ménard, R., 2008. Host cell traversal is important for progression of the malaria parasite

through the dermis to the liver. Cell Host Microbe 3, 88–96. doi:10.1016/j.chom.2007.12.007

Asada, M., Goto, Y., Yahata, K., Yokoyama, N., Kawai, S., Inoue, N., Kaneko, O., Kawazu, S., 2012. Gliding motility of *Babesia bovis* merozoites visualized by time-lapse video microscopy. PLoS One 7, e35227. doi:10.1371/journal.pone.0035227

Aurrecoechea, C., Barreto, A., Basenko, E.Y., Brestelli, J., Brunk, B.P., Cade, S., Crouch, K., Doherty, R., Falke, D., Fischer, S., Gajria, B., Harb, O.S., Heiges, M., Hertz-Fowler, C., Hu, S., Iodice, J., Kissinger, J.C., Lawrence, C., Li, W., Pinney, D.F., Pulman, J.A., Roos, D.S., Shanmugasundram, A., Silva-Franco, F., Steinbiss, S., Stoeckert, C.J., Spruill, D., Wang, H., Warrenfeltz, S., Zheng, J., 2017. EuPathDB: The eukaryotic pathogen genomics database resource. Nucleic Acids Res. 45, D581–D591. doi:10.1093/nar/gkw1105

Baran, K., Dunstone, M., Chia, J., Ciccone, A., Browne, K.A., Clarke, C.J.P., Lukoyanova, N., Saibil, H., Whisstock, J.C., Voskoboinik, I., Trapani, J.A., 2009. The molecular basis for perforin oligomerization and transmembrane pore assembly. Immunity 30, 684–695. doi:10.1016/j.immuni.2009.03.016

Bock, R., Jackson, L., de Vos, A., Jorgensen, W., 2004. Babesiosis of cattle. Parasitology 129, S247–S269. doi:10.1017/S0031182004005190

Brayton, K.A., Lau, A.O.T., Herndon, D.R., Hannick, L., Kappmeyer, L.S., Berens, S.J., Bidwell, S.L., Brown, W.C., Crabtree, J., Fadrosh, D., Feldblum, T., Forberger, H.A., Haas, B.J., Howell, J.M., Khouri, H., Koo, H., Mann, D.J., Norimine, J., Paulsen, I.T., Radune, D., Ren, Q., Smith Jr., R.K., Suarez, C.E., White, O., Wortman, J.R., Knowles Jr., D.P., McElwain, T.F., Nene, V.M., 2007. Genome sequence of *Babesia bovis* and comparative analysis of apicomplexan hemoprotozoa. PLoS Pathog. 3, e148. doi:10.1371/journal.ppat.0030148

Cornillot, E., Hadj-Kaddour, K., Dassouli, A., Noel, B., Ranwez, V., Vacherie, B., Augagneur, Y., Brès, V., Duclos, A., Randazzo, S., Carcy, B., Debierre-Grockiego, F., Delbecq, S., Moubri-Ménage, K., Shams-Eldin, H., Usmani-Brown, S., Bringaud, F., Wincker, P., Vivarès, C.P., Schwarz, R.T., Schetters, T.P., Krause, P.J., Gorenflot, A., Berry, V., Barbe, V., Mamoun, C.B., 2012. Sequencing of the smallest *Apicomplexan* genome from the human pathogen *Babesia microti*. Nucleic Acids Res. 40, 9102–9114. doi:10.1093/nar/gks700

693 Criado-Fornelio, A., Martinez-Marcos, A., Buling-Saraña, A., Barba-Carretero, J.C., 2003. Molecular studies
694 on Babesia, Theileria and Hepatozoon in southern Europe: Part II. Phylogenetic analysis and
695 evolutionary history. Vet. Parasitol. 114, 173–194. doi:10.1016/S0304-4017(03)00141-9
696 de Vries, E., Corton, C., Harris, B., Cornelissen, W.C.A., Berriman, M., 2006. Expressed sequence tag (EST)
697 analysis of the erythrocytic stages of *Babesia bovis*. Vet. Parasitol. 138, 61–74.
698 doi:10.1016/j.vetpar.2006.01.040
699 de Waal, D.T., Combrink, M.P., 2006. Live vaccines against bovine babesiosis. Vet. Parasitol. 138, 88–96.
700 doi:10.1016/j.vetpar.2006.01.042
701 Deligianni, E., Morgan, R.N., Bertuccini, L., Wirth, C.C., Silmon de Monerri, N.C., Spanos, L., Blackman, M.J.,
702 Louis, C., Pradel, G., Siden-Kiamos, I., 2013. A perforin-like protein mediates disruption of the
703 erythrocyte membrane during egress of *Plasmodium berghei* male gametocytes. Cell. Microbiol. 15,
704 1438–1455. doi:10.1111/cmi.12131
705 Deligianni, E., Silmon de Monerri, N.C., McMillan, P.J., Bertuccini, L., Superti, F., Manola, M., Spanos, L.,
706 Louis, C., Blackman, M.J., Tilley, L., Siden-Kiamos, I., 2018. Essential role of *Plasmodium* perforin-like
707 protein 4 in ookinete midgut passage. PLoS One 13, e0201651. doi:10.1371/journal.pone.0201651
708 Denton, J.F., Lugo-Martinez, J., Tucker, A.E., Schrider, D.R., Warren, W.C., Hahn, M.W., 2014. Extensive
709 error in the number of genes inferred from draft genome assemblies. PLoS Comput. Biol. 10,
710 e1003998. doi:10.1371/journal.pcbi.1003998
711 Dong, H., Xu, X., Deng, M., Yu, X., Zhao, H., Song, H., Geng, Y., 2007. Expression and bioactivity of
712 recombinant segments of human perforin. Biochem. Cell Biol. 85, 203–208. doi:10.1139/O07-017
713 Ecker, A., Pinto, S.B., Baker, K.W., Kafatos, F.C., Sinden, R.E., 2007. *Plasmodium berghei*: *Plasmodium*
714 perforin-like protein 5 is required for mosquito midgut invasion in *Anopheles stephensi*. Exp. Parasitol.
715 116, 504–508. doi:10.1016/j.exppara.2007.01.015
716 Eichenberger, R.M., Ramakrishnan, C., Russo, G., Deplazes, P., Hehl, A.B., 2017. Genome-wide analysis of
717 gene expression and protein secretion of *Babesia canis* during virulent infection identifies potential
718 pathogenicity factors. Sci. Rep. 7, e3357. doi:10.1038/s41598-017-03445-x
719 Elton, C.M., Rodriguez, M., Ben Mamoun, C., Lobo, C.A., Wright, G.J., 2019. A library of recombinant

Babesia microti cell surface and secreted proteins for diagnostics discovery and reverse vaccinology. Int. J. Parasitol. 49, 115–125. doi:10.1016/j.ijpara.2018.10.003

Fischer, S., Brunk, B.P., Chen, F., Gao, X., Harb, O.S., Iodice, J.B., Shanmugam, D., Roos, D.S., Stoeckert, C.J., 2011. Using OrthoMCL to assign proteins to OrthoMCL-DB groups or to cluster proteomes into new ortholog groups, in: Current Protocols in Bioinformatics. pp. 1–19. doi:10.1002/0471250953.bi0612s35

Florin-Christensen, M., Suarez, C.E., Rodriguez, A.E., Flores, D.A., Schnittger, L., 2014. Vaccines against bovine babesiosis: where we are now and possible roads ahead. Parasitology 141, 1563–1592. doi:10.1017/S0031182014000961

Garg, S., Agarwal, S., Kumar, S., Yazdani, S.S., Chitnis, C.E., Singh, S., 2013. Calcium-dependent permeabilization of erythrocytes by a perforin-like protein during egress of malaria parasites. Nat. Commun. 4, e1736. doi:10.1038/ncomms2725

Garg, S., Sharma, V., Ramu, D., Singh, S., 2015. *In silico* analysis of calcium binding pocket of perforin like protein 1: insights into the regulation of pore formation. Syst. Synth. Biol. 9, 17–21. doi:10.1007/s11693-015-9166-x

Garg, S., Shivappagowdar, A., Hada, R.S., Ayana, R., Bathula, C., Sen, S., Kalia, I., Pati, S., Singh, A.P., Singh, S., 2020. *Plasmodium* Perforin-like Protein pores on the host cell membrane contribute in its multistage growth and erythrocyte senescence. Front. Cell. Infect. Microbiol. 10, e121. doi:10.3389/fcimb.2020.00121

Goddard, T.D., Huang, C.C., Meng, E.C., Pettersen, E.F., Couch, G.S., Morris, J.H., Ferrin, T.E., 2018. UCSF ChimeraX: Meeting modern challenges in visualization and analysis. Protein Sci. 27, 14–25. doi:10.1002/pro.3235

Gohil, S., Herrmann, S., Günther, S., Cooke, B.M., 2013. Bovine babesiosis in the 21st century: advances in biology and functional genomics. Int. J. Parasitol. 43, 125–132. doi:10.1016/j.ijpara.2012.09.008

González, L.M., Estrada, K., Grande, R., Jiménez-Jacinto, V., Vega-Alvarado, L., Sevilla, E., De La Barrera, J., Cuesta, I., Zaballos, Á., Bautista, J.M., Lobo, C.A., Sánchez-Flores, A., Montero, E., 2019. Comparative and functional genomics of the protozoan parasite *Babesia divergens* highlighting the invasion and

egress processes. PLoS Negl. Trop. Dis. 13, 1–23. doi:10.1371/journal.pntd.0007680

Guerra, A.J., Carruthers, V.B., 2017. Structural features of apicomplexan pore-forming proteins and their roles in parasite cell traversal and egress. Toxins. 9, e265. doi:10.3390/toxins9090265

Guerra, A.J., Zhang, O., Bahr, C.M.E., Huynh, M.-H., DelProposto, J., Brown, W.C., Wawarzak, Z., Koropatkin, N.M., Carruthers, V.B., 2018. Structural basis of *Toxoplasma gondii* perforin-like protein 1 membrane interaction and activity during egress. PLoS Pathog. 14, e1007476. doi:10.1371/journal.ppat.1007476

Ishino, T., Chinzei, Y., Yuda, M., 2005. A *Plasmodium* sporozoite protein with a membrane attack complex domain is required for breaching the liver sinusoidal cell layer prior to hepatocyte infection. Cell. Microbiol. 7, 199–208. doi:10.1111/j.1462-5822.2004.00447.x

Jackson, A.P., Otto, T.D., Darby, A., Ramaprasad, A., Xia, D., Echaide, I.E., Farber, M., Gahlot, S., Gamble, J., Gupta, D., Gupta, Y., Jackson, L., Malandrin, L., Malas, T.B., Moussa, E., Nair, M., Reid, A.J., Sanders, M., Sharma, J., Tracey, A., Quail, M.A., Weir, W., Wastling, J.M., Hall, N., Willadsen, P., Lingelbach, K., Shiels, B., Tait, A., Berriman, M., Allred, D.R., Pain, A., 2014. The evolutionary dynamics of variant antigen genes in *Babesia* reveal a history of genomic innovation underlying host-parasite interaction. Nucleic Acids Res. 42, 7113–7131. doi:10.1093/nar/gku322

Jaramillo Ortiz, J.M., Molinari, M.P., Gravisaco, M.J., Paoletta, M.S., Montenegro, V.N., Wilkowsky, S.E., 2016. Evaluation of different heterologous prime–boost immunization strategies against *Babesia bovis* using viral vectored and protein-adjuvant vaccines based on a chimeric multi-antigen. Vaccine 34, 3913–3919. doi:10.1016/j.vaccine.2016.05.053

Kadota, K., Ishino, T., Matsuyama, T., Chinzei, Y., Yuda, M., 2004. Essential role of membrane-attack protein in malarial transmission to mosquito host. Proc. Natl. Acad. Sci. U. S. A. 101, 16310–16315. doi:10.1073/pnas.0406187101

Kafsack, B.F.C., Carruthers, V.B., 2010. Apicomplexan perforin-like proteins. Commun. Integr. Biol. 3, 18–23. doi:10.4161/cib.3.1.10076

Kafsack, B.F.C., Pena, J.D.O., Coppens, I., Ravindran, S., Boothroyd, J.C., Carruthers, V.B., 2009. Rapid membrane disruption by a perforin-like protein facilitates parasite exit from host cells. Science. 323, 530–533. doi:10.1126/science.1165740.Rapid

774 Kaiser, K., Camargo, N., Coppens, I., Morrisey, J.M., Vaidya, A.B., Kappe, S.H.I., 2004. A member of a
775 conserved *Plasmodium* protein family with membrane-attack complex/perforin (MACPF)-like domains
776 localizes to the micronemes of sporozoites. Mol. Biochem. Parasitol. 133, 15–26.
777 doi:10.1016/j.molbiopara.2003.08.009
778 Kawai, S., Igarashi, I., Abgaandorjiin, A., Miyazawa, K., Ikadai, H., Nagasawa, H., Fujisaki, K., Mikami, T.,
779 Suzuki, N., Matsuda, H., 1999. Ultrastructural characteristics of *Babesia caballi* in equine erythrocytes
780 *in vitro*. Parasitol. Res. 85, 794–799. doi:https://doi.org/10.1007/s004360050635
781 Kawai, S., Takahashi, K., Sonoda, M., Kurosawa, T., 1986. Ultrastructure of intra-erythrocytic stages of
782 *Babesia ovata*. Japanese J. Vet. Sci. 48, 943–949. doi:10.1292/jvms1939.48.943
783 Kumar, S., Stecher, G., Li, M., Knyaz, C., Tamura, K., 2018. MEGA X: Molecular evolutionary genetics analysis
784 across computing platforms. Mol. Biol. Evol. 35, 1547–1549. doi:10.1093/molbev/msy096
785 Kuo, C.H., Kissinger, J.C., 2008. Consistent and contrasting properties of lineage-specific genes in the
786 apicomplexan parasites *Plasmodium* and *Theileria*. BMC Evol. Biol. 8, e108. doi:10.1186/1471-2148-8-
787 108
788 Lawrence, J.G., 2005. Common themes in the genome strategies of pathogens. Curr. Opin. Genet. Dev. 15,
789 584–588. doi:10.1016/j.gde.2005.09.007
790 Levy, M.G., Ristic, M., 1980. *Babesia bovis*: Continuous cultivation in a microaerophilous stationary phase
791 culture. Science. 207, 1218–1220. doi:10.1126/science.7355284
792 Madeira, F., Park, Y.M., Lee, J., Buso, N., Gur, T., Madhusoodanan, N., Basutkar, P., Tivey, A.R.N., Potter,
793 S.C., Finn, R.D., Lopez, R., 2019. The EMBL-EBI search and sequence analysis tools APIs in 2019. Nucleic
794 Acids Res. 47, W636–W641. doi:10.1093/nar/gkz268
795 Mehlhorn, H., Schein, E., 1985. The Piroplasms: life cycle and sexual stages, in: Advances in Parasitology.
796 Academic Press, pp. 37–103. doi:10.1016/S0065-308X(08)60285-7
797 Moreno-Hagelsieb, G., Vitug, B., Medrano-Soto, A., Saier, M.H., 2017. The Membrane Attack
798 Complex/Perforin Superfamily. J. Mol. Microbiol. Biotechnol. 27, 252–267. doi:10.1159/000481286
799 Mossaad, E., Asada, M., Nakatani, D., Inoue, N., Yokoyama, N., Kaneko, O., Kawazu, S., 2015. Calcium ions
800 are involved in egress of *Babesia bovis* merozoites from bovine erythrocytes. J. Vet. Med. Sci. 77, 53–

58. doi:10.1292/jvms.14-0391

Ni, T., Williams, S.I., Rezelj, S., Anderluh, G., Harlos, K., Stansfeld, P.J., Gilbert, R.J.C., 2018. Structures of monomeric and oligomeric forms of the *Toxoplasma gondii* perforin-like protein 1. Sci. Adv. 4, eaaq0762. doi:10.1126/sciadv.aaq0762

Palmer, D.A., Buening, G.M., Carson, C.A., 1982. Cryopreservation of *Babesia bovis* for *in vitro* cultivation. Parasitology 84, 567–572. doi:https://doi.org/10.1017/S0031182000052835

Pedroni, M.J., Sondgeroth, K.S., Gallego-Lopez, G.M., Echaide, I., Lau, A.O.T., 2013. Comparative transcriptome analysis of geographically distinct virulent and attenuated *Babesia bovis* strains reveals similar gene expression changes through attenuation. BMC Genomics 14, e763. doi:10.1186/1471-2164-14-763

Potgieter, F.T., Els, H.J., 1977. The fine structure of intra-erythrocytic stages of *Babesia bigemina.* Onderstepoort J. Vet. Res. 44, 157–167.

Risco-Castillo, V., Topçu, S., Marinach, C., Manzoni, G., Bigorgne, A.E., Briquet, S., Baudin, X., Lebrun, M., Dubremetz, J.F., Silvie, O., 2015. Malaria sporozoites traverse host cells within transient vacuoles. Cell Host Microbe 18, 593–603. doi:10.1016/j.chom.2015.10.006

Rodriguez, S.D., Buening, G.M., Green, T.J., Carson, C.A., 1983. Cloning of *Babesia bovis* by *in vitro* cultivation. Infect. Immun. 42, 15–18.

Roiko, M.S., Carruthers, V.B., 2013. Functional dissection of *Toxoplasma gondii* perforin-like protein 1 reveals a dual domain mode of membrane binding for cytolysis and parasite egress. J. Biol. Chem. 288, 8712–8725. doi:10.1074/jbc.M113.450932

Roiko, M.S., Carruthers, V.B., 2009. New roles for perforins and proteases in apicomplexan egress. Cell. Microbiol. 11, 1444–1452. doi:10.1111/j.1462-5822.2009.01357.x

Roiko, M.S., Svezhova, N., Carruthers, V.B., 2014. Acidification activates *Toxoplasma gondii* motility and egress by enhancing protein secretion and cytolytic activity. PLoS Pathog. 10, e1004488. doi:10.1371/journal.ppat.1004488

Schreeg, M.E., Marr, H.S., Tarigo, J.L., Cohn, L.A., Bird, D.M., Scholl, E.H., Levy, M.G., Wiegmann, B.M., Birkenheuer, A.J., 2016. Mitochondrial genome sequences and structures aid in the resolution of

828 *Piroplasmida* phylogeny. PLoS One 11, e0165702. doi:10.1371/journal.pone.0165702
829 Suarez, C.E., Bishop, R.P., Alzan, H.F., Poole, W.A., Cooke, B.M., 2017. Advances in the application of genetic
830 manipulation methods to apicomplexan parasites. Int. J. Parasitol. 47, 701–710.
831 doi:10.1016/j.ijpara.2017.08.002
832 Suarez, C.E., McElwain, T.F., 2009. Stable expression of a GFP-BSD fusion protein in *Babesia bovis*
833 merozoites. Int. J. Parasitol. 39, 289–297. doi:10.1016/j.ijpara.2008.08.006
834 Suarez, C.E., Norimine, J., Lacy, P., McElwain, T.F., 2006. Characterization and gene expression of *Babesia*
835 *bovis* elongation factor-1α. Int. J. Parasitol. 36, 965–73. doi:10.1016/j.ijpara.2006.02.022
836 Templeton, T.J., Iyer, L.M., Anantharaman, V., Enomoto, S., Abrahante, J.E., Subramanian, G.M., Hoffman,
837 S.L., Abrahamsen, M.S., Aravind, L., 2004. Comparative analysis of *Apicomplexa* and genomic diversity
838 in Eukaryotes. Genome Res. 14, 1686–1695. doi:10.1101/gr.2615304
839 Ueti, M.W., Johnson, W.C., Kappmeyer, L.S., Herndon, D.R., Mousel, M.R., Reif, K.E., Taus, N.S., Ifeonu,
840 O.O., Silva, J.C., Suarez, C.E., Brayton, K.A., 2020. Comparative analysis of gene expression between
841 *Babesia bovis* blood-stages and kinetes allowed improved genome annotation. Int. J. Parasitol. Article
842 in press.
843 Voskoboinik, I., Thia, M.-C., Fletcher, J., Ciccone, A., Browne, K., Smyth, M.J., Trapani, J.A., 2005. Calcium-
844 dependent plasma membrane binding and cell lysis by perforin are mediated through its C2 domain. J.
845 Biol. Chem. 280, 8426–8434. doi:10.1074/jbc.M413303200
846 Wade, K.R., Tweten, R.K., 2015. The Apicomplexan CDC/MACPF-like pore-forming proteins. Curr. Opin.
847 Microbiol. 26, 48–52. doi:10.1016/j.mib.2015.05.001
848 Wilkowsky, S.E., Bareiro, G.G., Mon, M.L., Moore, D.P., Caspe, G., Campero, C., Fort, M., Romano, M.I.,
849 2011. An applied printing immunoassay with recombinant Nc-SAG1 for detection of antibodies to
850 *Neospora caninum* in cattle. J. Vet. Diagnostic Investig. 23, 971–976. doi:10.1177/1040638711416845
851 Wirth, C.C., Bennink, S., Scheuermayer, M., Fischer, R., Pradel, G., 2015. Perforin-like protein PPLP4 is
852 crucial for mosquito midgut infection by *Plasmodium falciparum*. Mol. Biochem. Parasitol. 201, 90–99.
853 doi:10.1016/j.molbiopara.2015.06.005
854 Wirth, C.C., Glushakova, S., Scheuermayer, M., Repnik, U., Garg, S., Schaack, D., Kachman, M.M., Weißbach,

T., Zimmerberg, J., Dandekar, T., Griffiths, G., Chitnis, C.E., Singh, S., Fischer, R., Pradel, G., 2014. Perforin-like protein PPLP2 permeabilizes the red blood cell membrane during egress of *Plasmodium falciparum* gametocytes. Cell. Microbiol. 16, 709–733. doi:10.1111/cmi.12288

Yamagishi, J., Asada, M., Hakimi, H., Tanaka, T.Q., Sugimoto, C., Kawazu, S., 2017. Whole-genome assembly of *Babesia ovata* and comparative genomics between closely related pathogens. BMC Genomics 18, 832. doi:10.1186/s12864-017-4230-4

Yang, A.S.. P., O'Neill, M.T., Jennison, C., Lopaticki, S., Allison, C.C., Armistead, J.S., Erickson, S.M., Rogers, K.L., Ellisdon, A.M., Whisstock, J.C., Tweedell, R.E., Dinglasan, R.R., Douglas, D.N., Kneteman, N.M., Boddey, J.A., 2017. Cell traversal activity is important for *Plasmodium falciparum* liver infection in humanized mice. Cell Rep. 18, 3105–3116. doi:10.1016/j.celrep.2017.03.017

Yang, J., Zhang, Y., 2015. I-TASSER server: New development for protein structure and function predictions. Nucleic Acids Res. 43, W174–W181. doi:10.1093/nar/gkv342

869 **Legends to figures**

870 **Figure 1: Multiple sequence alignment of *B. bovis* PLP1 and its orthologs *T. gondii* PLP1 and *P. falciparum***
871 **PLP1 and PLP3.** The 20 amino acids of the MACPF motif are underlined in orange, and the 4 cysteine
872 residues of each of the three repeats of the APC-β domain are indicated with a red star. Blue arrows show
873 the two residues (G866 and E868) of the *B. bovis* PLP1 predicted Ca^{2+} binding site. Amino acids are colored
874 according to their physicochemical features using the Clustal color scheme. In all alignments, aminoacids
875 that are conserved in at least 75% of the sequences are colored-shaded.

876 **Figure 2. Phylogenetic analysis of the MACPF domain of *Babesia* PLPs.** Amino acid sequences of the
877 MACPF domain of each PLP were used for inferring a tree by the Maximum Likelihood method. Bootstrap
878 values are shown next to branches. The MACPF domain of PLP1 of *Toxoplasma gondii* RH (ABK97634.2) was
879 included as outgroup.

880 **Figure 3. Predicted structure of *B. bovis* PLP1.** A. Schematic representation of the domains in *B. bovis* PLP1.
881 SP denotes the signal peptide and gray rectangles show each of the direct tandem repeats of the APC-β
882 domain. B. 3D model of the complete protein. C. 3D model of the MACPF (left) and APC-β (right) domains.
883 α-helixes are shown in pink while β-strands are shown in yellow. In the MACPF domain, the characteristic
884 clusters of α-helixes (CH1 and CH2) surrounding the antiparallel chains that form the twisted β-sheet are
885 indicated in circles. D. Bottom view of the APC-β domain shown in Figure 4c (left) and detail of the position
886 of the four conserved cysteine residues with the predicted disulfide bridges (yellow lines) that are formed
887 between them in each of the repeats (right). E. A Hidden Markov Model consensus of a single APC-β repeat
888 from all *Babesia* PLPs showing conservation of the four cysteine residues (grey arrows).

889 **Figure 4. Patterns of transcription of *B. bovis plp* genes.** Number of normalized reads obtained by RNA
890 sequencing for the transcripts of each of the *B. bovis plp* genes in kinete and merozoite stages (A) and in
891 blood stages of a virulent strain and its attenuated derivative (B).

892 **Figure 5. Hemolysis assays of rPLP1_MACPF.** A. Lysis of bovine erythrocytes using a constant concentration
893 (100 nM) of protein. B. Dose-response curve using increasing concentrations of protein. C. pH-dependent
894 hemolysis using 100 nM of rPLP1_MACPF. D. Hemolysis assay using 100 nM of protein in variable Ca^{2+}
895 concentration. In all cases hemolysis was expressed as a percentage of maximum hemoglobin release with

1% Triton X-100 treatment. An unrelated protein of *N. caninum* (rSAG) expressed and purified as rPLP1_MACPF was used as negative control. *$p < 0.001$ with one-way ANOVA and Dunnett post-test. C- denotes negative control.

Figure 6. Microscopic observation of *B. bovis* transfected cultures. A. Control culture transfected with pBluesctipt. B and C. Knock out culture transfected with pBbo*Δplp1,* 5- or 15-days post transfection (dpt). Upper panels: Smears stained with Diff Quik. Lower panels: transfected parasites under fluorescent light. Scale-bars: 10 µm.

Figure 7. PCR assays to assess the disruption of *plp1* by integration of the *egfp-bsd* selectable marker. PCR amplifications were done on genomic DNA extracted from: the S74-T3Bo strain (1), cultures of *Δplp1* strain from two independent transfections (2 and 3), S74-T3Bo culture 2 days post transfection with pBluescript (4), plasmid pBbo*Δplp1* (5), negative control (6). *msa1* gene was amplified to verify the integrity of the DNA.

Figure 8. Fluorescence microscopy of *Δplp1* and e*Δplp1* cultures. Parasites stained with Hoechst 33342 from the *B. bovis Δplp1* culture before (*Δplp1*) and after enrichment (e*Δplp1*) by FACS. Scale-bar: 10 µm.

Figure 9. Flow cytometry analysis of the enriched culture e*Δplp1.* Hydroethidine stained cells (yellow fluorescence) and eGFP expressing cells (green fluorescence) of the enriched line (e*Δplp1*), the S74-T3Bo wild type parasites and two artificial mixtures in different proportions (1:1 and 10:1) of e*Δplp1*: S74-T3Bo were analyzed by flow cytometry. Yellow and green fluorescence are indicated in the corresponding axes.

Figure 10. Phenotypic evaluation of e*Δplp1*. A. Comparative *in vitro* growth curve of *B. bovis* S74-T3Bo (WT) and e*Δplp1* lines. The assay was done in triplicate wells and data are expressed as arithmetic means ± standard deviation. *$p < 0.05$ with a Student's t-test. B. Unusual tetrads observed in *B. bovis Δplp1* cultures. Culture smears of e*Δplp1* and WT lines were stained with Diff Quik and observed under light microscope (1000X, upper panel). Arrows indicate RBC containing more than a pair of merozoites. Scale-bars: 10 µm. A digital magnification of an RBC containing a tetrad is shown in the lower panel.

Supplementary Fig. S1. Schematic representation of the *B. bovis plp1* locus and the transfection plasmid pBbo*Δplp1*. A. Structure of the *plp1* gene locus in the wild type strain. B. Transfection plasmid pBbo*Δplp1.* The ef-1α promoter that controls the expression of the *egfp-bsd* gene and the 3'- region of the *rap-1* gene

are shown in white while 5´and 3´UTR are shown in grey. C. Structure of the resulting locus after homologous recombination in the *plp1* knock out strain.

Supplementary Fig. S2. Schematic representation of PCR assays to evaluate integration of the *egfp-bsd* gene in the *plp1* locus. PCR primers are indicated as arrows and their numbers correspond to those indicated in Supplementary Table S2. * indicates that primers hybridize in gDNA sequences that are not included in the transfection plasmid pBbo*Δplp1*.

Supplementary Fig. S3. Multiple sequence alignment of the six *B. bovis* PLPs. The complete MACPF domain is underlined in orange and the wider line denotes the 20 amino acids of the conserved motif. Amino acids are colored according to their physicochemical features using the Clustal color scheme.

Supplementary Fig. S4. Multiple sequence alignment of the MACPF domain of all *Babesia* PLPs. The 20 amino acids of the conserved motif are underlined in orange. Amino acids are colored according to their physicochemical features using the Clustal color scheme.

Supplementary Fig. S5. Multiple sequence alignment of the APC-β domain of all *Babesia* PLP in which this domain was found. The stars indicate the four conserved cysteine residues of the three tandem repeats. Amino acids are colored according to their physicochemical features using the Clustal color scheme.

Supplementary Fig. S6. Synteny of the PLP *loci* between *Babesia* species. The dotted lines indicate the location of the PLP orthologs in other *Babesia* species. Conservation of surrounding genes is shown as shaded areas.

Supplementary Fig. S7. Structure of MACPF domains of all *B. bovis* PLPs. In all the cases the two clusters of α-helixes on both sides of the antiparallel β-strands that form a β-sheet are evident.

Supplementary Fig. S8. Conservation of the tertiary structure of *B. bovis* PLP1 and its functional domains. A. Overlap of the model of complete *B. bovis* PLP1 (colors) and the structure corresponding to the C6 protein of the human complement system (grey, PDB: 3t5o). B. Overlap of the model of the MACPF domain of *B. bovis* PLP1 (colors) and the structure of the lymphocyte perforin (grey, PDB: 3nsj). C. Overlap of the model of the APC-β domain of *B. bovis* PLP1 (colors) and the structure corresponding to the APC-β domain of *T. gondii* PLP1 (grey, PDB: 6d7a). In all the cases, the secondary structure of the *B. bovis* protein was colored based on the secondary structure (α-helixes in pink and β-strands in yellow).

Supplementary Fig. S9. PLP1 is expressed by *B. bovis* blood stages during bovine infection. A. Western blot analysis of a *B. bovis* merozoite lysate using (1) pre-immune, (2) anti RAP-1, (3) anti rPLP1_MAPCF polyclonal mouse sera. B. Western blot analysis of rPLP1_MACPF using sera from (1) non-infected cattle, (2) naturally *B. bovis* infected cattle, (3) mouse polyclonal anti rPLP1 serum and (4) commercial anti his-tag. All reactions were developed using a colorimetric method with the exception on lane 3 on figure A that was developed using chemiluminescence. The black arrow indicates the expected molecular weight of the complete *B. bovis* PLP1 protein.

Supplementary Fig. S10. Quantitative PCR assays on cDNA from the wild type and the enriched *Δplp1* line. Relative quantification of *plp1* transcription in the wild type S74-T3Bo strain (WT) and in the enriched *Δplp1* line (e*Δplp1*).

Tables

Table 1: PLPs identified in the different species of *Babesia*. aa, amino acids. Chr., chromosome. NA, genes not assigned to chromosomes since the genome is not assembled to that level. SP, signal peptide. TM, transmembrane domain. [a] indicates proteins with multiple MACPF domains. [b] indicates positions in amino acids.

Species	Class of PLP	Locus tag	Protein length (aa)	# Exons	Chr.	SP[b]	MACPF[b]	TM[b]	APC-β
B. bovis T2B	PLP1	BBOV_IV001370	978	1	4	1-25	422-646	694-711	Yes
	PLP2	BBOV_II007150	752	1	2	-	518-744	553-572; 615-638	No
	PLP3[a]	BBOV_III000410	1272	17	3	1-21	247-423; 548-700; 1076-1255	763-784; 837-854	Yes
	PLP4	BBOV_II002020	420	7	2	1-22	183-371	282-301	No
	PLP5	BBOV_II001970	559	8	2	1-21	157-354	142-162; 442-459	Yes
	PLP6	BBOV_III000320	512	6	3	-	99-294	326-343; 479-512	Yes
B. ovata Miyake	PLP1	BOVATA_036650	1057	1	NA	-	552-777	788-808; 897-917	Yes
	PLP2	BOVATA_023240	1004	1	NA	-	767-992	856-875	No
	PLP3	BOVATA_042350	424	3	NA	1-21	206-419	-	No
	PLP4	BOVATA_032330	604	10	NA	1-19	178-396	-	Yes
	PLP6	BOVATA_042230	536	6	NA	1-20	145-330	400-422	Yes
	PLP8	BOVATA_042310	592	8	NA	-	353-575	186-210	No
B. bigemina BOND	PLP1	BBBOND_0402480	966	1	4	-	462-686	807-826	Yes
	PLP2	BBBOND_0103080	1206	1	1	1-21	972-1197	934-953	No
	PLP3	BBBOND_0301750	450	4	3	1-21	247-445	211-235	No
	PLP4	BBBOND_0202000	696	9	2	1-25	181-399	-	Yes
	PLP5	BBBOND_0201960	651	6	2	1-15	154-386	247-268; 288-310; 474-491; 599-615	Yes
	PLP6	BBBOND_0301590	563	7	3	1-25	146-340	-	Yes

	PLP7	BBBOND_0301700	637	10	3	1-24	159-373	470-494; 520-536	Yes
	PLP8	BBBOND_0301690	386	6	3	-	129-351	-	No
B. divergens 1802A	PLP1	Bdiv_013880c	894	2	NA	-	387-613	-	Yes
	PLP2	Bdiv_014980	513	2	NA	-	269-494	-	No
	PLP3	Bdiv_018170c	460	4	NA	1-21	259-454	263-282	No
	PLP4	Bdiv_011150	660	11	NA	1-29	178-396	263-281; 445-463;	Yes
	PLP5	Bdiv_011160c	610	12	NA	1-21	152-366	480-498; 593-610	Yes
	PLP6	Bdiv_018050c	562	7	NA	1-23	140-339	269-290	Yes
	PLP7	Bdiv_018160c	621	11	NA	1-28	172-377	541-562	Yes
	PLP8	Bdiv_018150c	364	6	NA	-	121-342	528-553	No
B. microti RI	PLP1	BMR1_02g00320	879	6	2	1-21	347-575	336-354; 613-633; 706-722	Yes
	PLP2	BMR1_01G03475_2	352	4	1	-	131-346	216-235	No
	PLP3[a]	BMR1_04g09590	982	12	4	-	42-252; 356-584; 751-970	835-853	No
	PLP4	BMR1_01G02875	614	12	1	1-21	133-365	-	Yes
	PLP5	BMR1_01G02876	357	4	1	1-21	121-336	-	No
	PLP6	BMR1_04g09550	504	8	4	-	109-317	-	Yes
B. canis BcH-CHIPZ	PLP1	Bc-CHIPZ-H003086	602	-	NA	1-18	420-598	-	No
	PLP2	Bc-CHIPZ-H001240	371	-	NA	-	179-362	-	No
	PLP3	Bc-CHIPZ-H001168	259	-	NA	-	123-241	-	No
	PLP8	Bc-CHIPZ-H001159	164	-	NA	-	19-147	-	No

966

Figure

Click here to access/download;Figure;Figure 1 - Color.jpg

Figure

Click here to access/download;Figure;Figure 2.jpg

Figure

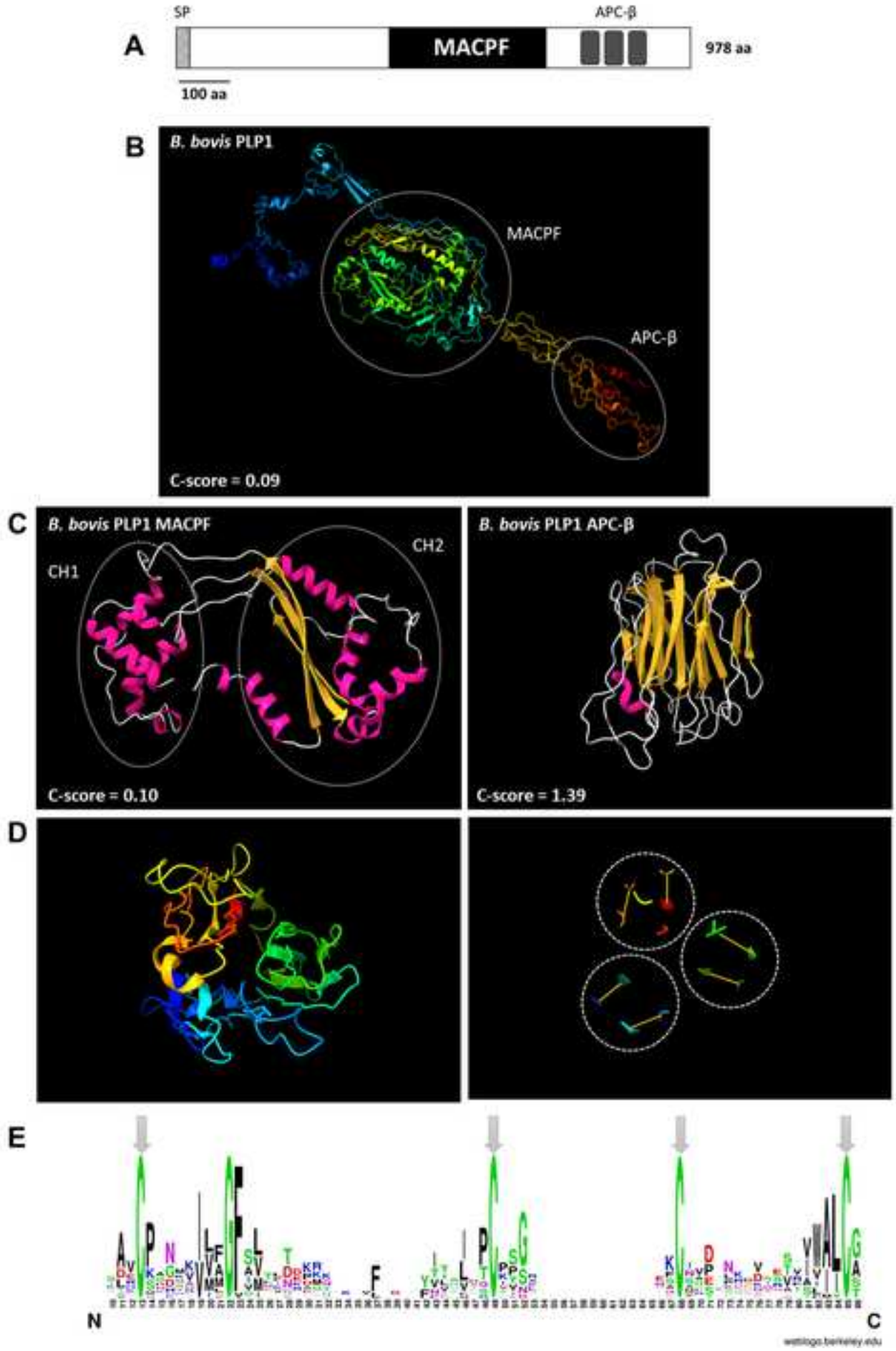

Figure

Click here to access/download;Figure;Figure 4.jpg

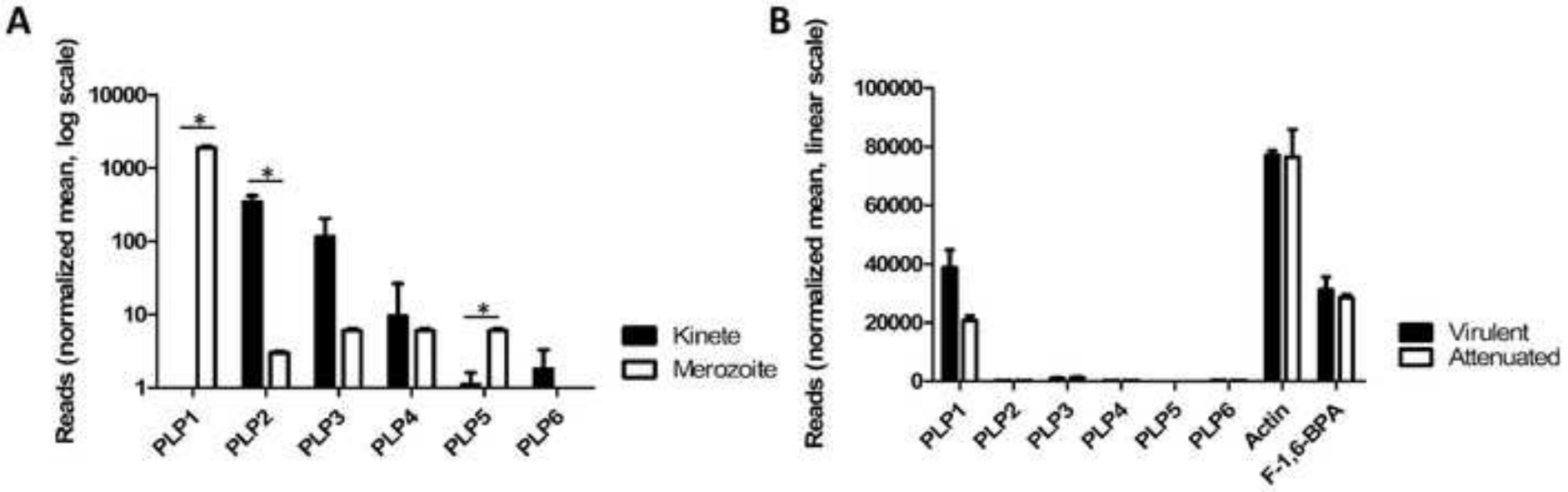

Figure

Click here to access/download;Figure;Figure 5.jpg

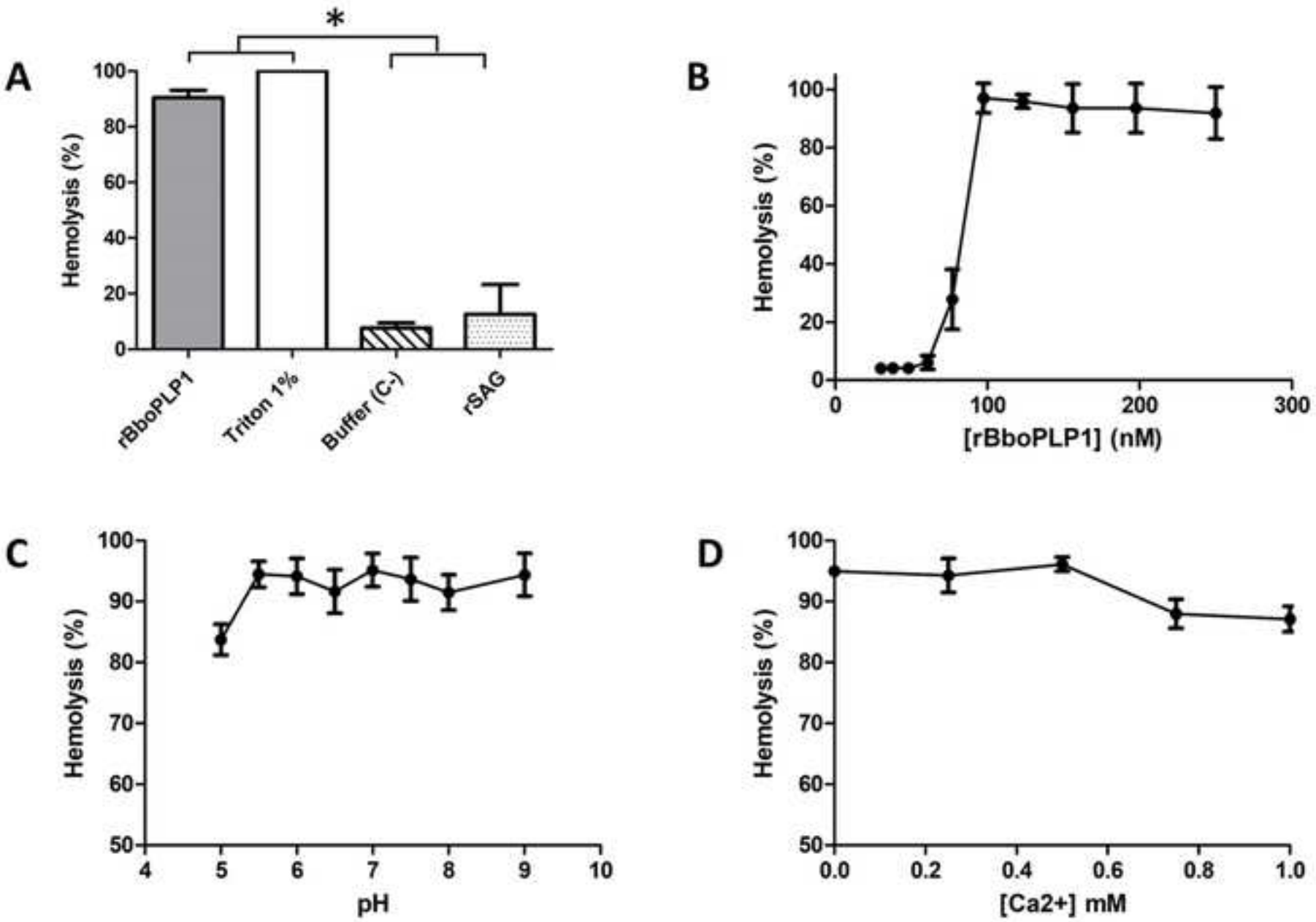

Figure

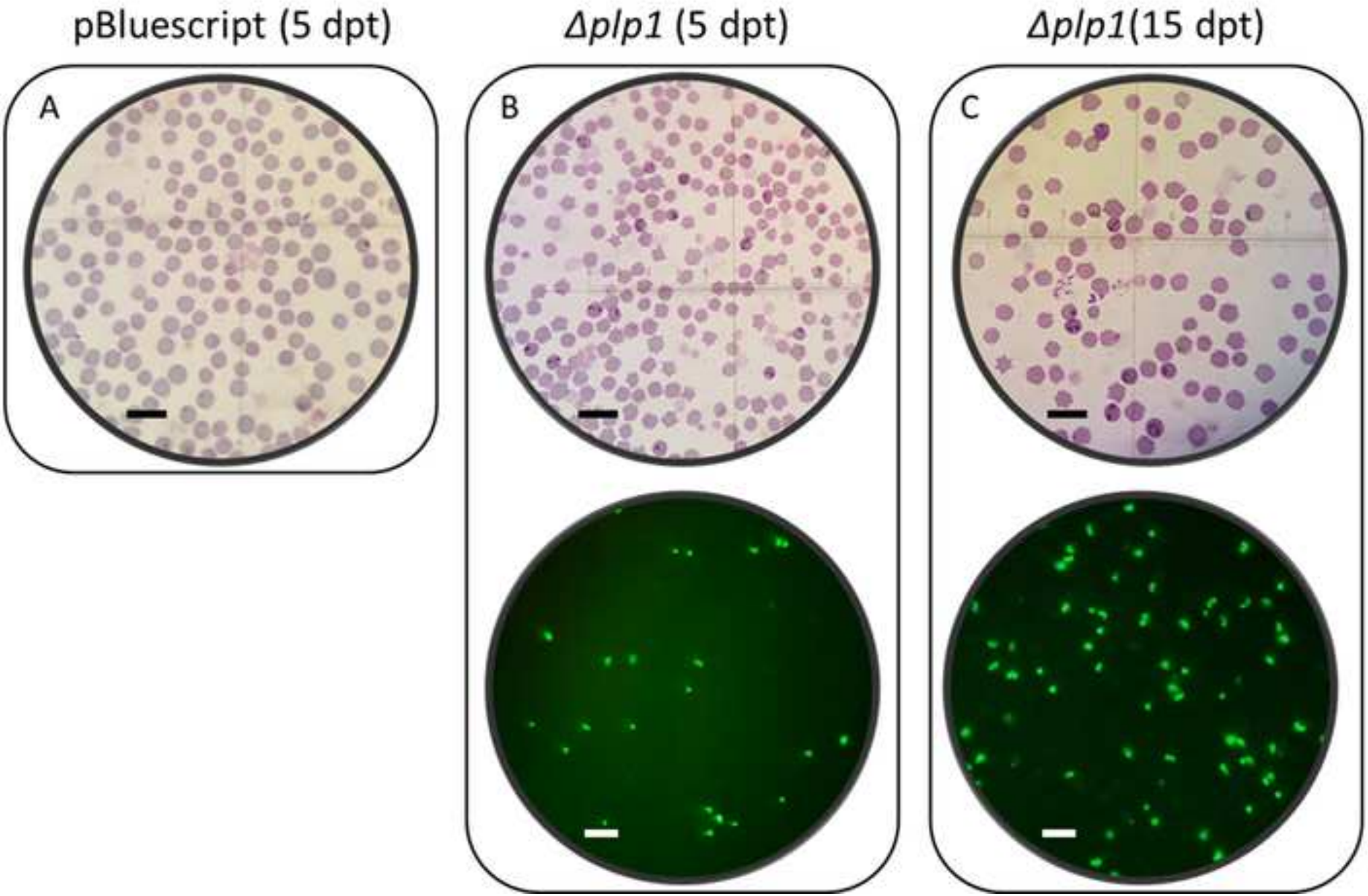

Figure

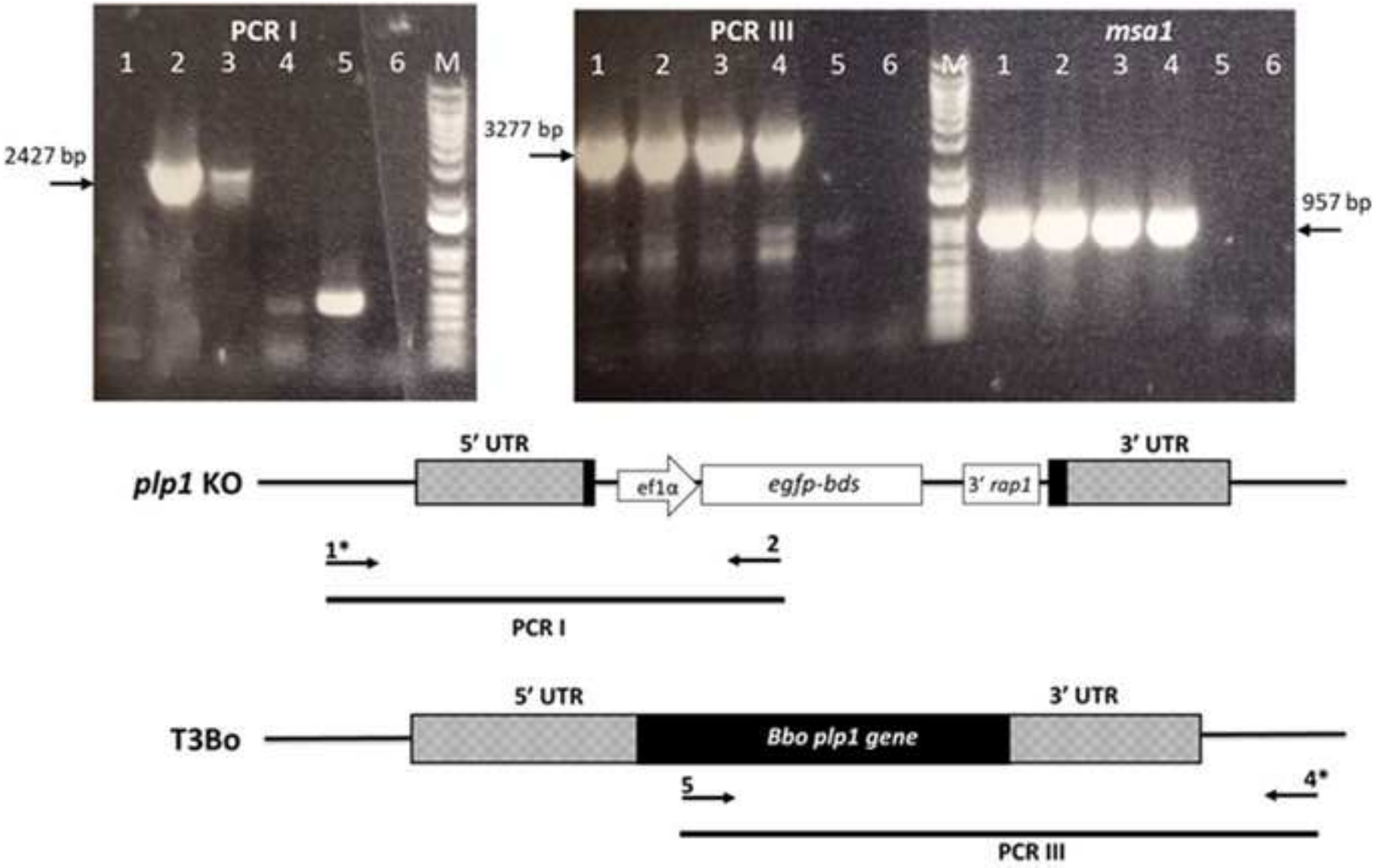

Figure

Click here to access/download;Figure;Figure 8 - Color.jpg

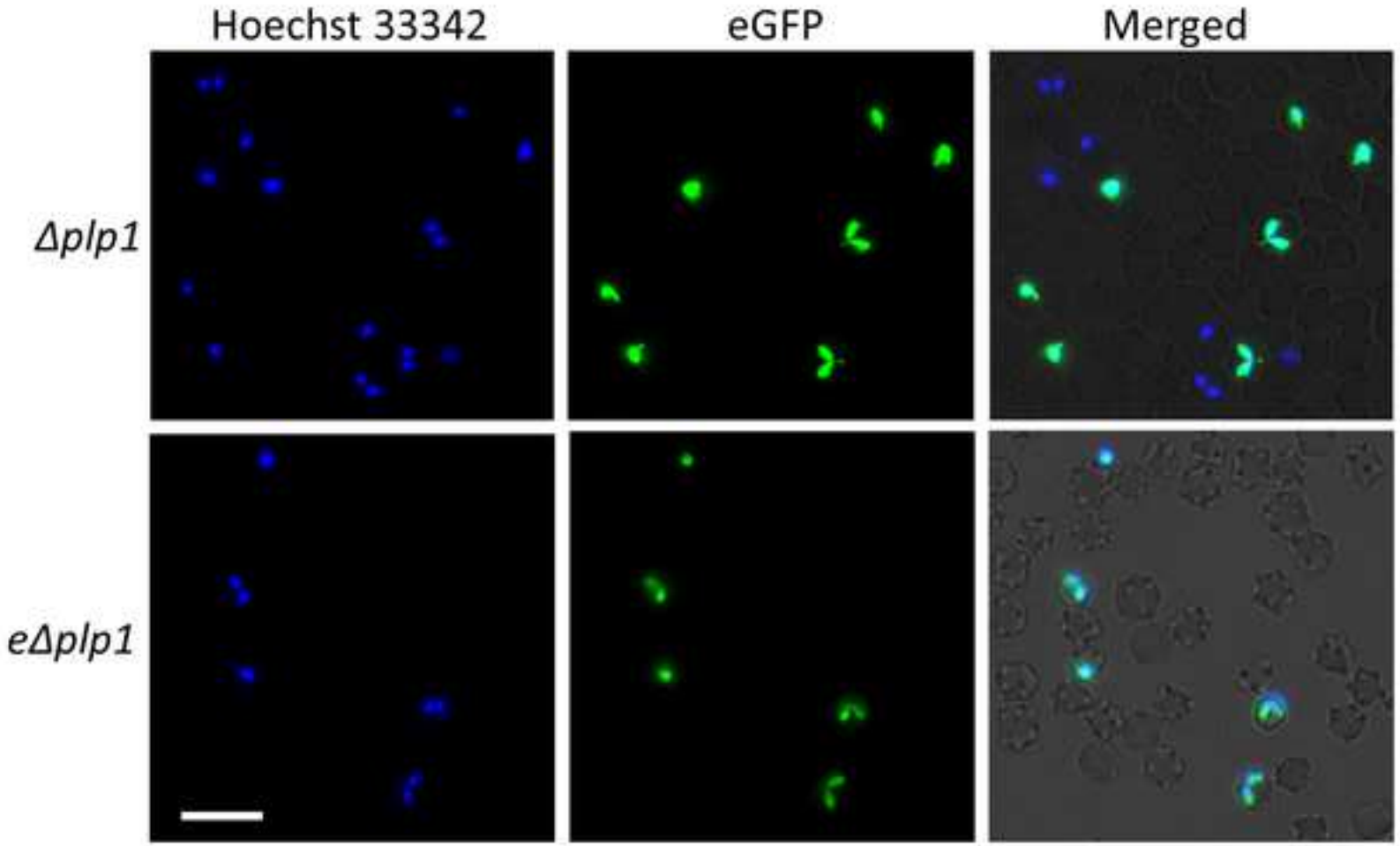

Figure

Click here to access/download;Figure;Figure 9.jpg

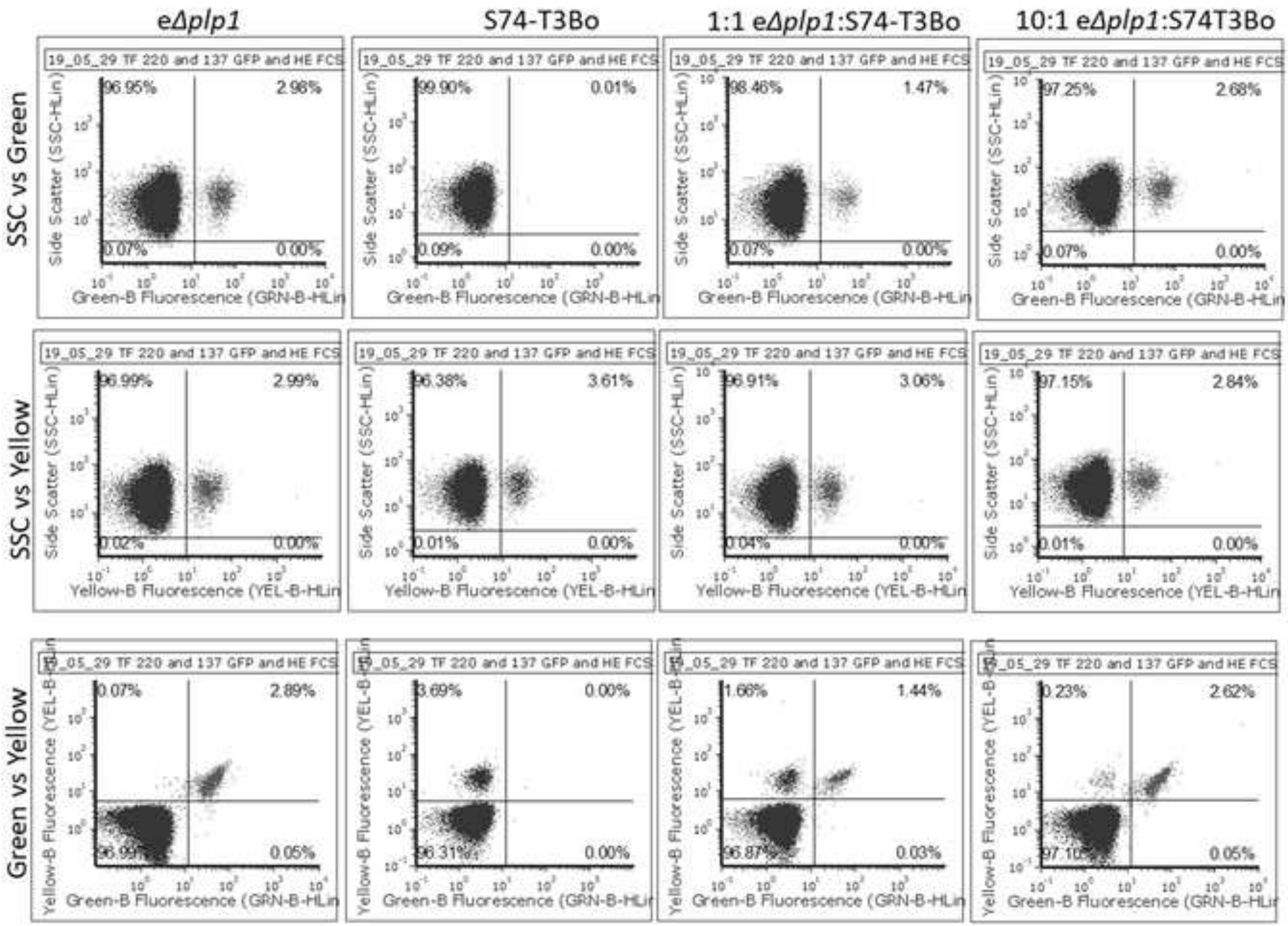

Figure

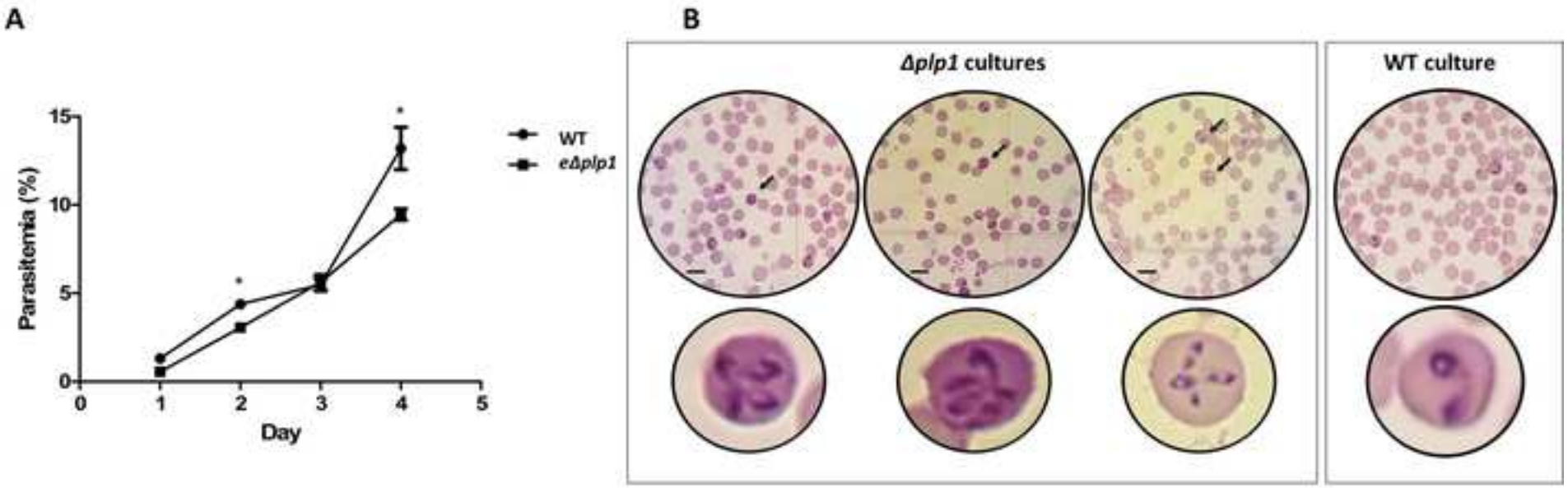

Supplementary figures